1970

A study of the design and construction of a full scale aircraft component demonstration fatigue test

Stephen Andrew Wright

Department:

A STUDY OF THE DESIGN AND CONSTRUCTION OF A FULL SCALE AIRCRAFT COMPONENT DEMONSTRATION FATIGUE TEST

BY

STEPHEN ANDREW WRIGHT, 1945-

A

THESIS

submitted to the faculty of

UNIVERSITY OF MISSOURI - ROLLA

in partial fulfillment of the requirements for the

Degree of

MASTER OF SCIENCE IN MECHANICAL ENGINEERING

Rolla, Missouri

1970

Approved by

Terry F. Lehnhoff (advisor) Robert L. Davis

Ralph E. Schowalter

ABSTRACT

The objective of this project was to design and build a full scale demonstration fatigue test for a Piper Aztec stabilator. A general discussion of the construction is included in this report.

The Fourier series method of the aerodynamic theory of spanwise loading was used to determine the load distribution. The results show a close relationship with data furnished by Piper Aircraft Corporation.

Fatigue theory is discussed in order to provide background for fatigue testing. The test specimen, methods and procedures of testing, known loading methods and systems, safety, etc., are discussed.

Federal requirements for regulating and testing of aircraft are reviewed. Approved methods of obtaining the distribution of load are included.

ACKNOWLEDGEMENT

Special thanks are extended to Dr. T. L. Lehnhoff, Dr. R. T. Johnson, and Mr. R. D. Smith. Dr. Lehnhoff, the author's advisor, provided the initial encouragement and guidance required to produce this thesis. Dr. Johnson made suggestions leading to the development of the load control system. Mr. Smith helped with the construction of the apparatus for the test.

Thanks are also given to Mr. Fred C. Stashak, Chief Stress Engineer at Piper Aircraft Corporation, and Mr. Richard Cover of Beech Aircraft Corporation.

The author is grateful for the support and understanding given to him by his wife, Susan, and his mother, Virginia Wright, who typed the thesis.

TABLE OF CONTENTS

Page

ABSTRACT ii

ACKNOWLEDGEMENT iii

LIST OF ILLUSTRATIONS vi

LIST OF TABLES vii

NOTATION viii

I. INTRODUCTION 1

II. REVIEW OF LITERATURE 3

A. AERODYNAMIC THEORY 3

1. Methods of Obtaining Spanwise Load Distribution . . 13

2. Methods of Obtaining Chordwise Distribution 19

B. FATIGUE THEORY AND METHODS 19

1. The Test Specimen 22

2. Test Loading 22

3. Testing Methods 23

4. Applied Loading Method 25

5. Testing Procedures 25

C. AIRWORTHINESS REQUIREMENTS AND REGULATIONS 26

1. Fatigue Requirements 26

2. Airplane Airworthiness Requirements 27

a. Load Distribution in the Spanwise Direction . . 27

b. Load Distribution in the Chord Direction 28

c. Resultant Air Loads on a Wing 28

III. DISCUSSION 29

A. DETERMINING THE AERODYNAMIC LOAD DISTRIBUTION 29

1. Load Distribution in the Spanwise Direction 29

Page

2. Load Distribution in the Chord Direction 51

B. STABILATOR TEST CONSTRUCTION 51

1. Stabilator Mounting 51

2. Whiffletree Design 54

3. Loading System and Control 55

IV. CONCLUSIONS AND RECOMMENDATIONS 59

V. BIBLIOGRAPHY 60

VI. VITA 62

LIST OF ILLUSTRATIONS

Figures		Page
1.	Vortex Circulation of Flow	5
2.	Finite Wing Span Showing Vortex Circulation	6
3.	Location of Point P from Vortex Line AB	7
4.	Downwash Velocities of a Wing	8
5.	Actual Lift Distribution Along a Wing Span	9
6.	Three Horseshoe-Shaped Vortex Systems to Approximate the Actual Lift Distribution About a Wing	10
7.	Location of the Trailing Vortex and the Downwash Velocity	11
8.	Relationship of the Angles of Attack	12
9.	Cyclic Loading Actions	23
10.	Lift Distribution Obtained from the Fourier Series Analysis	42
11.	Horizontal Tail Surface Pad Locations Used by Piper Aircraft Corporation	43
12.	Piper Spanwise Whiffletree Design	45
13.	Comparison of the Lift Distribution in Plane C	48
14.	Stabilator Pad Locations Used in Thesis Project	49
15.	Thesis Whiffletree Design	50
16.	Tail Surface Load Distribution in the Chord Direction	53
17.	Stabilator Test System	54
18.	Whiffletree System	55
19.	Pressure Control System	56
20.	Control Loading System	57
21.	Loading Air Cylinder and Whiffletree	58

LIST OF TABLES

		Page
I.	Geometric Characteristics of the Piper Stabilator	30
II.	Computing Form for Evaluating Angle Coefficients, B_n . . .	31
III.	Computing Form for Evaluating Plan Form Coefficients C_{2n} .	33
IV.	Stabilator Calculation Form for the C_{2n} Coefficients . . .	34
V.	Stabilator Solution of the A_n Coefficients	36
VI.	Stabilator Computation of the Coefficient of Lift Ratio . .	38
VII.	Stabilator Computation of the Load Distribution	39
VIII.	Piper Whiffletree Dimensions	46
IX.	Piper Design of the Spanwise Load Distribution	47
X.	Thesis Project Design of the Spanwise Load Distribution . .	47
XI.	Thesis Whiffletree Dimensions	52
XII.	Computation Form for the Chordwise Distribution	53

NOTATION

A	Aspect ratio of wing $= \frac{b^2}{S}$
A_n	Coefficients of the Fourier series of the Lotz method equations
α_a	The absolute angle of attack
α_i	Induced angle of attack or $\tan \alpha_i = \frac{w}{V}$
α_o	Effective angle of attack at any point along the span
b	Total wing span from tip to tip
β	Angle between velocity vector, υ, on the path of integration and the tangent to the path
B_n	Coefficients of the Fourier series of the Lotz method equations
c	Chord of wing
c_l	Coefficient of lift at a point on the wing span
C_L	Average or constant wing lift coefficient along entire wing span
c_s	Chord length between the extended trailing edge and leading edge at centerline of aircraft
C_{2n}	Coefficients of the Fourier series of the Lotz method equations (even term coefficients)
$\frac{c_l}{C_L}$	Ratio of the lift coefficients at a particular point
δ_i	Average value of the ratio of the lift coefficients at the mid-point of a wing section
Γ	A constant for all points and is called the circulation
h_i	Average value of the chord length at the mid-point of a wing section
L	Lift per unit length
m_o	Slope of lift curve (c_l vs α_o) in radians
m_s	Slope of the lift curve for the airfoil at centerline of aircraft

ΔP_z	Load acting upon a particular wing section
r	Distance from center of vortex
ρ	Absolute density of the air
ds	Increment length of the path
S	Wing area (tip to tip)
θ	An angle measured on a circle having the radius of b/2
θ'	The particular value of theta corresponding to the coordinate y'
(TL)	Total load applied to the semispan
R_L	Reference lift in psi
υ	Flow velocity
V	Air velocity perpendicular to the tangent of the vortex
w	Downwash velocity which changes the direction of flow at the airfoil by a very small angle, α_i, called the induced angle of attack
y	Distance of the vortex center from the centerline of aircraft (see Figure 7)
y'	Distance from centerline of aircraft to the considered downwash velocity (see Figure 7)
Δy_i	Width of a wing section

I. INTRODUCTION

Since December 17, 1903, at Kitty Hawk, North Carolina, when Orville Wright first flew an aircraft under complete control using its own power, aviation technology has rapidly progressed. With this development, however, a number of problems have manifested themselves.

One major problem is fatigue. In the past twenty years this area of investigation has become of great importance. The reasons for this importance are many. The airlines now utilize a greater percentage of the life-span of an aircraft under flight conditions. Their operating procedures have changed by making speeds higher, approaching the design speed limits on older aircraft. The demands made on military aircraft have brought about the need for high design stresses. Because of larger aircraft with increased gross load capacities, new materials have been used in recent years which, while having less weight per unit volume, also have low residual static strength. However, with some new materials fatigue properties have not been improved. Fatigue failures of airline and military aircraft during flight have necessitated the requirement of fatigue testing prior to and after production (8)*.

Fatigue testing has been costly, taking up much time and floor space for aircraft companies, but it plays an important role in the design and maintenance of the aircraft.

The requirements set up for overall fatigue durability by various designers can be broken down into three general areas. The first is safe-life. This idea has been emphasized by European countries. Safe-life can be considered the estimated mean life of all aircraft of a

---

* Numbers in parentheses refer to reference numbers in the bibliography.

particular type in terms of flight hours, based on the fatigue tests given to the aircraft. The second concept is fail-safe design. This has been used primarily by American designers. The method requires the designer to insure that fatigue does not develop in an area which would be critical to structural strength to the point of disaster. The last concept is infinite life. This approach, from a performance viewpoint, is impractical because of weight penalties involved when designing for an expected infinite life without fatigue (8).

Many areas of fatigue that have not been studied may have to be investigated in the future. Such areas of fatigue as those caused by elevated temperatures and sonic effects are examples of problems needing further investigation.

In the light of the preceding discussion it seems evident that a study of the various areas which must be considered in the design of a full scale aircraft fatigue test should be worthwhile. This is even more evident when one considers the fact that the method of loading is the only feature which distinguishes an aircraft fatigue test from most other structural fatigue tests. Thus, this study has more universal application than might be immediately obvious.

For this project a suitable structural test component was necessary. After initial contacts were made with several companies, a Piper Aztec (light twin engine aircraft) stabilator was donated by Piper Aircraft Corporation. The test was to be designed and constructed in such a manner that it would represent closely the methods that aircraft manufacturers employ.

II. REVIEW OF LITERATURE

A. AERODYNAMIC THEORY

In this project the author has designed and set up a full scale demonstration fatigue test on a Piper Aztec horizontal stabilator. In order to understand the aerodynamic theory involved for a stabilator, the following excerpt will be helpful. The excerpt explains the function of a stabilator and the differences between a stabilator and the horizontal stabilizer of a conventional tail.

> The principal aim of the aeronautical engineer is the reduction of drag and weight. Designers seek also a reduction in complexity--in the number of individual parts that must be manufactured and attached to one another. The stabilator responds to these requirements: Because its entire surface reacts effectively against the airstream, whereas only a portion of the total area of a conventional tail does so, a stabilator may be smaller than a conventional tail to achieve a given degree of control effectiveness, or it may give better effectiveness for a certain size. Not only can it be made smaller (and hence lighter and less draggy), but it may also be made with fewer parts. The well-designed stabilator therefore represents an improvement over the two- or three-part horizontal tail.
>
> It consists simply of a single slab, usually cut away in the center to make way for the fuselage, with a small torque box carrying through the fuselage and holding the two sides of the stabilator rigidly in the same plane with respect to one another. The trailing edge, or a portion of it, is equipped with a narrow flap called an antiservo tab, which moves in the same direction as the rear half of the stabilator; thus, "up stabilator" (trailing edge up, corresponding to "up elevator") produces "up tab."
>
> The whole thing is pivoted around its own 24- or 25-percent-of-chord point, usually on bolts in brackets attached to the rear fuselage bulkhead. By pivoting about its own center of lift (which is always right around 25 percent of chord), the stabilator is neutral in pitch; that is to say, without the antiservo tab, it would just sit any which way with respect to the airstream. The purpose of the tab is to make the stabilator line itself up with the airstream. By deflecting upward when the trailing edge of the surface rises, it pushes it back downward; deflecting downward against "down stabilator," it pushes the trailing edge of the stabilator back upward. In fact, the tab is always pushing one way or another, except when the tab is exactly aligned with the rest

> of the surface; the stabilator therefore tends always to return to and maintain this alignment. The stabilator/tab combination may be said to be "stable"; push it out of alignment, and the antiservo tab pushes it back.[1]

Theory has been developed by aerodynamicists to predict performance, control characteristics, stability, and other design criteria. The load distribution which can be obtained theoretically is needed by the stress analyst for internal structural design. For any theoretical analysis of the air load distribution, correct assumptions must be made for accurate analysis. Shear force and bending moment variations can be obtained from a load distribution analysis.

The spanwise distribution may depend upon the shape of the airfoil, the type of airfoil section used, and the position and dimensions of the trim tab (16).

In order to more clearly understand spanwise load distribution, the development will begin with wing vortex theory. This vortex theory has been taken from reference (16).

Figure 1 shows the circulation or flow about the center of the vortex. The wing downwash velocities can be obtained from a consideration of the circulation theory of lift. The tangential velocity at any point in the fluid is inversely proportional to the distance r of the point from the center of the vortex cylinder, or

$$\upsilon = \frac{\Gamma}{2\pi r} \tag{1}$$

---

[1]Peter Garrison, "Stabilators," Flying, January 1970, p. 62.

where Γ is constant for all points and is called the circulation. The units for the circulation constant can be considered as an area flow rate.

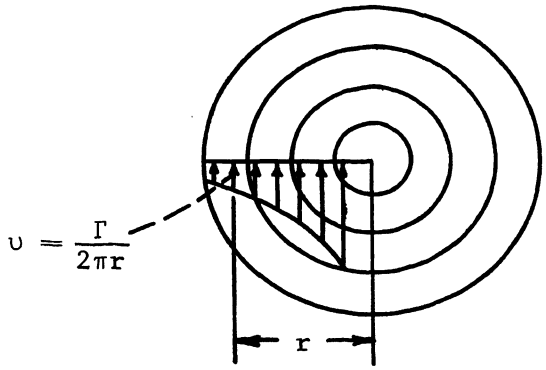

Figure 1. Vortex Circulation of Flow

The lift L per unit length is represented by the equation

$$L = \rho V \Gamma \tag{2}$$

The circulation for two dimensional flow is

$$\Gamma = \int \upsilon \cos \beta \, ds \tag{3}$$

The integration may be about any closed path in the plane.

In Figure 2 a finite wing span is shown. The vortex circulation does not end at the wing tips but extends for a considerable distance downstream which is assumed to be infinite. The strength of the vortex is considered to be constant along the line.

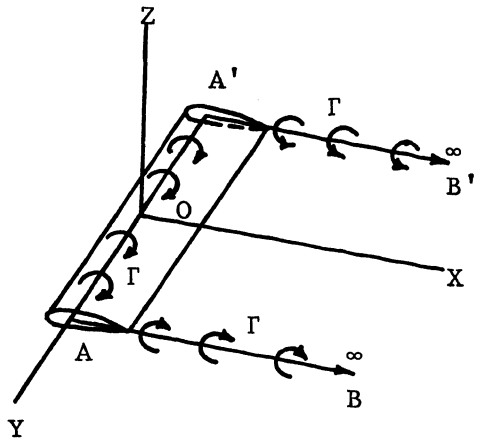

Figure 2. Finite Wing Span
Showing Vortex Circulation

Consider Point P in Figure 3. Point P is a distance r from the vortex line AB.

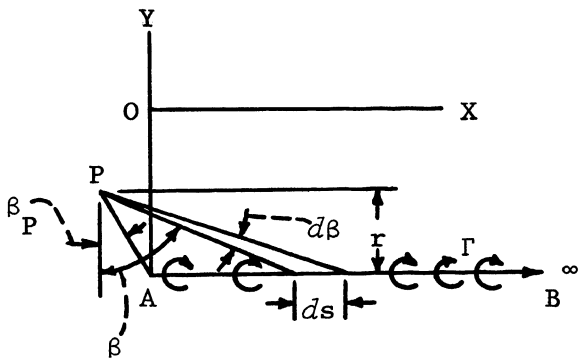

Figure 3. Location of Point P from Vortex Line AB

The contribution of the elementary length ds of the vortex line to the downwash velocity at Point P is shown by

$$dw = \frac{\Gamma}{4\pi r} \cos \beta \, d\beta \tag{4}$$

Then at Point P the downwash velocity is

$$w = \frac{\Gamma}{4\pi r} \int_{\beta_P}^{\frac{\pi}{2}} \cos \beta \, d\beta \tag{5}$$

For the entire wing span both vortices at the wing tips must be considered. The downwash velocity at some distance downstream from the wing is shown in Figure 4.

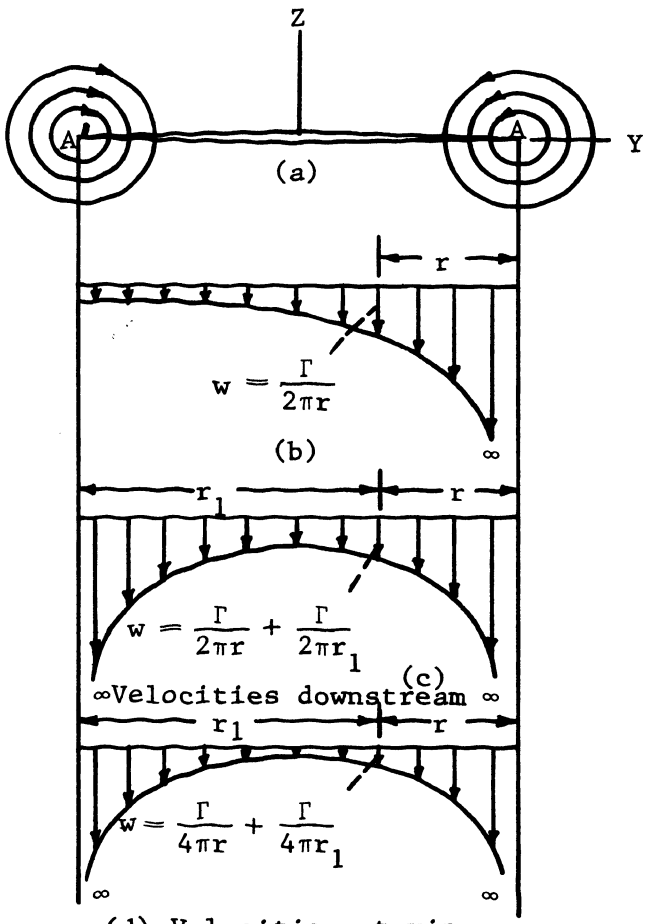

Figure 4. Downwash Velocities of a Wing

The downwash velocity of the wing span AA' of Figure 2 will be half of the downwash velocity shown in Figure 4(c), which is a point at a great distance downstream. This means that half of the final downwash velocity is attained at the wing, and at some great distance upstream from the wing the downwash velocity is zero.

Referring to Figure 5, it can be seen that the actual lift distribution along the wing span is represented by a curve instead of being a constant distribution as indicated by Figure 2. The letter q in Figure 5 is dynamic pressure.

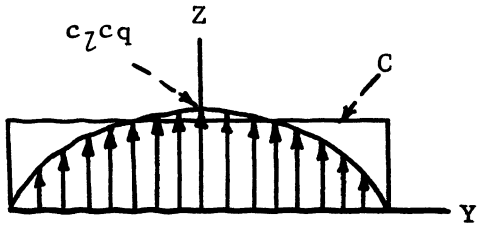

Figure 5. Actual Lift Distribution Along a Wing Span

In order to approximate the lift distribution closely, a number of horseshoe-shaped vortex systems may be combined, as shown in Figure 6.

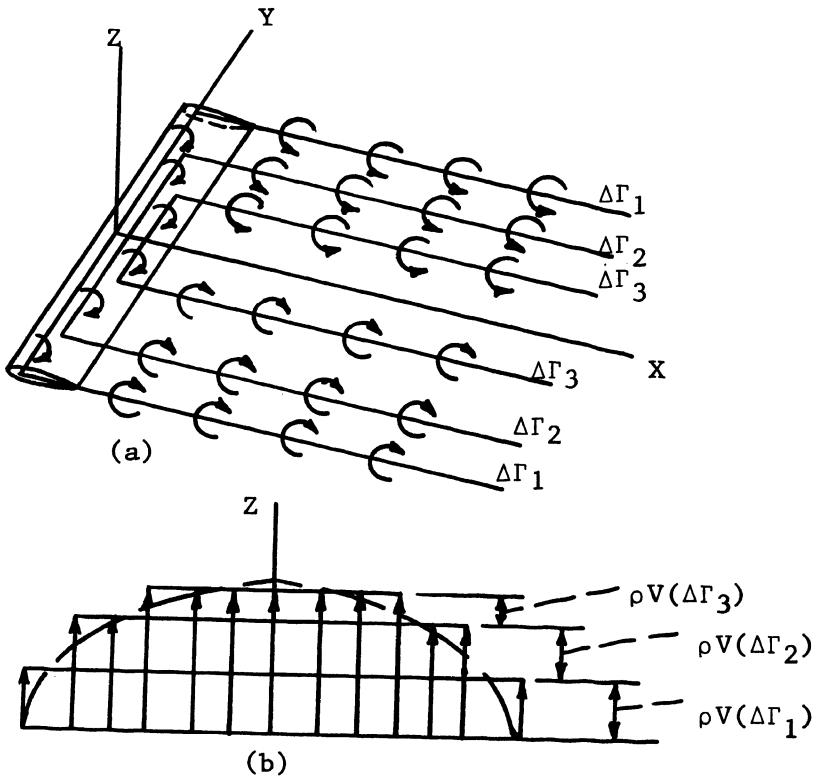

Figure 6. Three Horseshoe-Shaped Vortex Systems to Approximate the Actual Lift Distribution About a Wing

An infinite number of horseshoe vortices must be used to obtain the true vortex system. The downwash velocity equations may be developed by integrating the effect of all of these horseshoe systems. The trailing vortex is shown at Point y in Figure 7. At a fixed Point y' along the span the downwash velocity resulting from $d\Gamma$ is

$$dw = \frac{d\Gamma}{4\pi r} \tag{6}$$

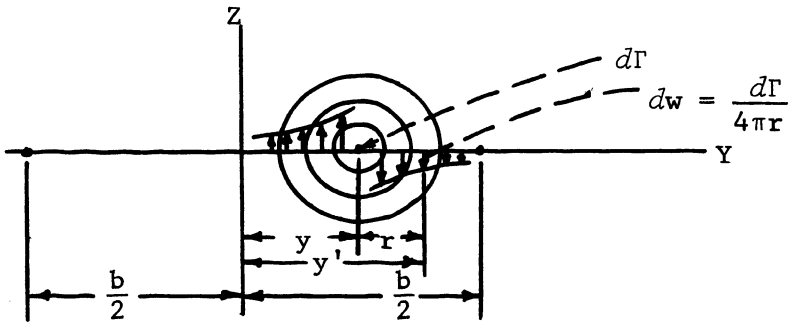

Figure 7. Location of the Trailing Vortex and the Downwash Velocity

The distance r is the distance of Point y' from the vortex center. The total downwash velocity, w, at the Point y' is the sum of the downwash velocities caused by all of the trailing vortices for the entire wing span. With all terms as a function of the distance y, this total downwash velocity is

$$w = \frac{1}{4\pi} \int_{y=-\frac{b}{2}}^{y=\frac{b}{2}} \frac{d\Gamma}{y'-y} \tag{7}$$

The lift coefficient, c_l, is equal to $m_o\alpha_o$ at a point o.

α_o is the effective angle of attack at any point along the span, or $\alpha_a - \alpha_i$. The relationship between the above angles of attack can be seen in Figure 8.

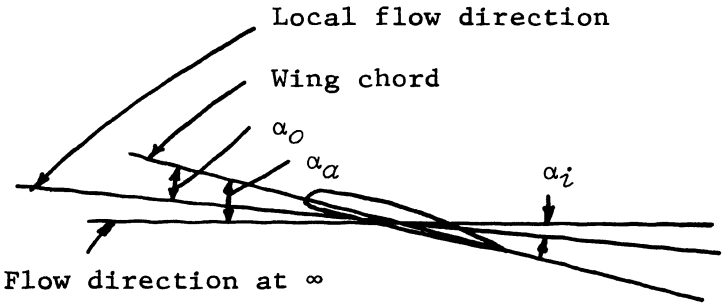

Figure 8. Relationship of the Angles of Attack

Then it follows that

$$c_l = m_o \alpha_o = m_o \left(\alpha_a - \frac{w}{V}\right) \tag{8}$$

The relationship between the circulation, Γ, and c_l is obtained by equating the lift on a wing section of unit span and chord c (see Equation 2).

$$c_l \frac{\rho V^2}{2} c = \rho V \Gamma \tag{9}$$

or

$$\Gamma = \frac{c_l c V}{2} \tag{10}$$

and from Equations 8 and 10

$$\Gamma = \frac{cVm_o}{2} \left(\alpha_a - \frac{w}{V}\right) \tag{11}$$

Eliminating the downwash velocity term w

$$\frac{2\Gamma}{m_o cV} = \alpha_a - \frac{1}{4\pi V} \int_{-\frac{b}{2}}^{\frac{b}{2}} \frac{d\Gamma}{y'-y} \tag{12}$$

and in terms of the lift coefficient, c_l

$$\frac{c_l}{m_o} = \alpha_a - \frac{1}{8\pi} \int_{y=-\frac{b}{2}}^{y=\frac{b}{2}} \frac{d(cc_l)}{y'-y} \tag{13}$$

The last two equations represent the fundamental equations for the spanwise distribution of the circulation, Γ.

1. Methods of Obtaining Spanwise Load Distribution

Determining the spanwise load distribution is important for structural considerations, stall characteristics and performance in the areas of angle of zero lift, pitching moment of the entire wing about the aerodynamic center, and induced drag. Reference (15) gives a number of variables concerned with load distribution because of twist, as follows:

(1) Wing angle of attack

(2) Flap type

(3) Flap span

(4) Flap deflection

(5) Wing plan form

(6) Variation of flap-chord ratio along the span

In this work twist has not been considered.

Spanwise load distribution is a linear function of the angle of attack at each point along the span.

A very good method for computing an approximate load distribution with 72 wing flap combinations is available in reference (15). In this reference, tables are given for simplifying the calculations.

A number of other methods have been developed to calculate an approximate spanwise load distribution on a wing. Some of these have been accepted by the Civil Aeronautics Manual (4). These approved methods will be mentioned in another section. Reference (17) contains an approved approximation.

In Aircraft Structures by Peery (16), an approximation using an elliptical plan form is available. An elliptical plan form has no aerodynamic twist. This means that zero-lift chords at all sections lie in a plane, the absolute angle of attack is the same at all sections along the span, and the slope of the lift curve will be constant along the span. This elliptical plan form produces minimum drag characteristics. Thus, a well designed wing will not vary greatly from the elliptical plan form.

In using this method, a direct solution for obtaining the lift coefficient values along the span is not possible. Thus, an initial value of the average lift coefficient must be assumed, and used in an equation

to find the values of the lift coefficient along the span. These coefficients can be verified by substitution and will be in terms of the assumed constant value of the lift coefficient along the entire span. In this same reference is given an approximation method for determining the lift distribution for twisted wings, and various flap conditions.

When calculating the coefficient of lift by the approximation methods, it is often convenient to compute separately the zero lift distribution due to the flaps, and then the distribution due to an angle of attack with neutral flaps. These can be superimposed in any combination to obtain desired conditions.

In order to obtain a more accurate distribution, the author has resorted to the Fourier series method. This method will give an accurate solution with any plan form, and is accepted by the Civil Aeronautics Manual. This method was necessary because it was found that the Piper Aztec stabilator did not follow in close enough form the physical properties needed to use one of the approximate methods.

The Fourier series method was first proposed by Glauert (7) and was further developed by Miss Lotz (14).

A brief discussion of this method and a simple mathematical procedure to obtain the coefficients has been written by Shenstone (18). Tabular form solutions which are readily used with a computer can be found in ANC-1(1) (1) and an article by Pearson (15). For the purposes of this thesis the author has used the tabulated forms in reference (15), for ten points along the span.

The circulation of a symmetrically loaded wing at any point along the span can be represented by the following series:

$$\Gamma = \sum_{n=1,3,5}^{\infty} a_n \cos \frac{n\pi y}{b} \tag{14}$$

The series may be written in the more convenient form

$$\Gamma = \frac{c_s m_s V}{2} \sum_{n=1}^{\infty} A_n \sin n\theta \tag{15}$$

$$\cos \theta = \frac{y}{b/2} \tag{16}$$

This last equation may be used for symmetric or unsymmetric loading. For the condition of symmetric loading, the even coefficients are zero.

The angle θ can be considered as an angle measured on a circle having a radius of b/2. The first term of Equation 15 will be proportional to the ordinates of the points on this circle.

The coefficients A_n of the series may be calculated by using the Fourier series values for the circulation, Γ, in Equation 12. Differentiating Equation 15 gives

$$d\Gamma = \frac{c_s m_s V}{2} \sum_{n=1}^{\infty} nA_n \cos n\theta \, d\theta \tag{17}$$

The last term which is the downwash angle or the induced angle of attack of Equation 12 can be obtained from Equations 16 and 17. It will now be

$$\alpha_i = \frac{c_s m_s}{4\pi b} \int_o^\pi \frac{\sum_{n=1}^{\infty} nA_n \cos n\theta \, d\theta}{\cos \theta - \cos \theta'} \tag{18}$$

noting that

$$\int_o^\pi \frac{\cos n\theta \, d\theta}{\cos \theta - \cos \theta'} = \frac{\pi \sin n\theta'}{\sin \theta'} \tag{19}$$

the downwash angle is

$$\alpha_i = \frac{c_s m_s}{4b} \frac{\sum_{n=1}^{\infty} nA_n \sin n\theta}{\sin \theta} \tag{20}$$

Equation 12 may now be written as

$$\frac{m_s c_s}{m_o c} \Sigma A_n \sin n\theta = \alpha_a - \frac{m_s c_s}{4b} \frac{\Sigma n A_n \sin n\theta}{\sin \theta} \tag{21}$$

or

$$\frac{m_s c_s}{m_o c} \sin \theta \Sigma A_n \sin n\theta = \alpha_a \sin \theta - \frac{m_s c_s}{4b} \Sigma n A_n \sin n\theta \tag{22}$$

The slope of the lift curve, m_o, the wing chord, c, and the angle of attack, α_a, all may vary along the span. To represent a wing of any shape, these terms may be expressed by other Fourier series, as follows:

$$\frac{m_s c_s}{m_o c} \sin \theta = \sum_{n=0,1,2,3}^{\infty} C_{2n} \cos 2n\theta \tag{23}$$

and

$$\alpha_a \sin \theta = \sum_{n=1,2,3}^{\infty} B_n \sin n\theta \tag{24}$$

The coefficients of these Fourier series may be found from known wing characteristics using a tabular format.

Equation 21 or 22 is considered the general equation for the circulation and represents the solution to the problem of obtaining the spanwise air-load distribution. These equations, along with Equations 23 and 24, can be arranged for tabular solution as mentioned above.

2. Methods of Obtaining Chordwise Distribution

Theoretical distribution methods in the chordwise direction have been developed but generally approximate methods are considered accurate enough to use in design. Tables for calculating the actual distribution are available in ANC-1(3) "Chordwise Air Load Distribution of Airfoils" (2). Severe loads in high speed airplanes, which generally act on the leading edge, and special loading such as parasite drag and propeller thrust, may be accounted for by methods outlined in NACA Report No. 413.

For purposes of this thesis, approximate methods were used, as outlined by references (4) and (5). These approximation methods will be discussed in another section.

B. FATIGUE THEORY AND METHODS

There are three general approaches to the fatigue problem. They are full scale testing, component testing, and theoretical as well as experimental engineering improvement. These approaches play important roles in the design of dependable aircraft.

Between the years 1939 and 1959, 200 to 300 full scale fatigue tests on aircraft structures had been run. Generally only one test was used per aircraft design because of cost limitations. This fatigue test had to be used to obtain both safe-life and fail-safe characteristics.

In designing full scale tests a number of considerations had to be investigated.

Considerations in Designing Full-Scale Tests

- Expected load experience
- Number of loading stations
- Method of loading
- Number of stress levels
- Loading sequence
- Disposition of cracks (8)

Concerning component testing, separate tests can be run on ribs, skin, spars, fittings, control surfaces, landing gear, and other critical components. One advantage of this type of testing is that the part can be tested at any time during construction or design. Other noteworthy factors are things such as less floor space, lower expense, less designing for the test itself, easier inspection, etc.

Engineering improvement may be readily understood from the following list of contributions:

Contributions from Fundamental Engineering Approach

- Material comparisons
- Alternating-mean stress relations
- Cumulative damage
- Notch effects
- Crack propagation
- Residual static strength
- Ways of improving fatigue behavior
- Environmental effects (8)

Fatigue prevention methods also include periodic inspections during the testing. The most logical method of inspection is by visual means. Other methods are X-rays, eddy currents, ultra-sonic techniques, dye penetrants, photographic techniques, magniflux, etc.

A general comparison of fatigue testing by constant level loading versus randomized-step type tests should be made. The random load test is more realistic and shows more fatigue sensitive areas (9). Often fatigue cracks are not in the same location when the two methods are compared.

> No one level in the constant-level tests consistently gave a good indication of the area which proved critical in the randomized-step tests. ...study indicates that the added complication of a randomized-step loading is warranted by the greater relevance of the fatigue-sensitive area indications to flight operations.[2]

Full scale fatigue tests can be used to obtain the values of the fatigue ratio which is used in design (12). The ratio is defined as the ratio of fatigue resistance to tensile strength under static loads. This ratio helps to evaluate properties of materials subject to fatigue. A structure will have many values of the ratio dependent upon the number of cycles and the type of loading applied during the fatigue tests. This ratio is important because it enables the designer to determine if the structure needs improvements or if noticeable concentrations of stresses are present in the structure.

---

[2]Wilber B. Huston, "Comparison of Constant-Level and Randomized-Step Tests of Full-Scale Structures as Indicators of Fatigue-Critical Components," Full Scale Fatigue Testing of Aircraft Structures, edited by F. J. Plantema and J. Schijve, Pergamon Press, 1961, p. 146.

The following five sections are subjects covered in a lecture given by W. J. Winkworth (19) on testing equipment and procedures.

1. The Test Specimen

The test specimen must be structurally complete which means that it should be an actual service aircraft, not a prototype. A prototype could be used for static testing but should not be used for fatigue testing unless the prototype is exactly like the production aircraft. If a prototype were used for the fatigue test, fatigue cracks could develop in different locations and be of a different type than if the service aircraft were used. This is extremely important for future service inspection schedules.

The use of half-span wing tests (partial component tests) are not desirable when a full span test is feasible. Minor changes in the design of the structure can greatly affect the fatigue life of an aircraft.

2. Test Loading

Desirable test loads are the kind that most nearly represent the actual service conditions.

> Broadly speaking, there are two main types: transport aircraft and combat aircraft. For transport aircraft, the loads must represent the transition from ground to air and also the turbulence met in flight. In the case of military aircraft the manoeuvres and turbulence met in flight must be represented and usually in the form of repeated programmes {see Figure 9}...
>
> The representation of the pressure loads in the fuselage is a further well-known example.
>
> Since full-scale tests are usually made to obtain fatigue strength data which can be directly applied to identical service aircraft, the requirement in this context is that the magnitudes and programming of the test loads must

accurately represent the conditions of use of the service aircraft.[3]

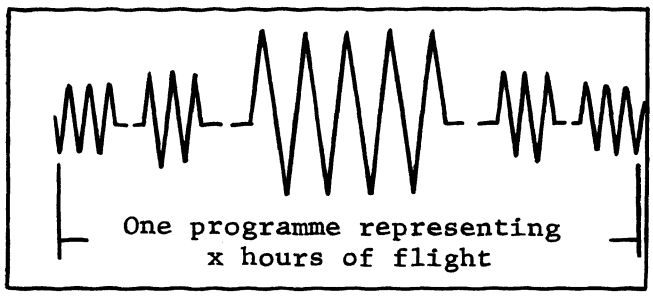

Fatigue test programme (Combat aircraft)

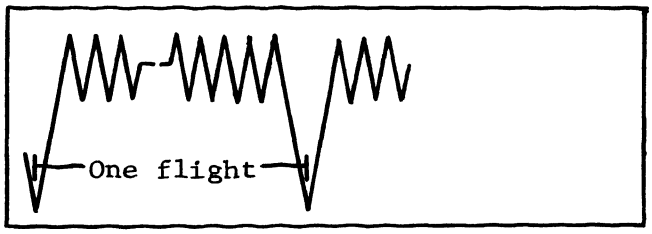

Simulated fatigue test flight (Transport aircraft)

Figure 9. Cyclic Loading Actions

3. Testing Methods

The testing methods can be divided into system functions. They are representation, application, and control.

It is not possible to attain absolute representation, and approximate means have therefore to be accepted.

---

[3]W. J. Winkworth, "The Fatigue Testing of Aircraft Structures," Full Scale Fatigue Testing of Aircraft Structures, edited by F. J. Plantema and J. Schijve, Pergamon Press, 1961, pp. 211-212.

> The requirements in this respect are for accurate representation of the spanwise condition of Bending Moment, Shear, and Torque.
>
> The chordwise conditions are represented approximately.
>
> Justification of this attitude is based on the following reasons. First, the vital conditions from the fatigue aspect are the spanwise bending moments and shears and these are accurately simulated. Secondly, the chordwise conditions are amenable to component testing techniques, for example a wing rib or a section of leading edge structure can be fatigue tested in this manner. Thirdly, the interaction between spanwise and chordwise conditions is usually minor.[4]

The main importance concerning application is not the actual magnitude of an applied load but the range between cyclic loading of major and minor loads. In fatigue loading the rate of cycling is sometimes important. Loading at different stations or locations of hydraulic loading cylinders must usually be in phase, especially in fatigue testing where the cyclic rate may be great. The response characteristics of the system are in direct proportion to the speed of the testing.

Some of the more important requirements in the control features of the system are as follows:

(1) Generally alternating loading

(2) Prevention of overloading

(3) Automatic control of cycling

(4) Accurate control with desired conditions, especially at the peaks and troughs in the cycle

(5) Sinusoidal characteristics and speed control are secondary because of relative slow loading rates.

(6) Devices required for sequence in cycling, control of load magnitude, and cycling rate

---

[4]Winkworth, pp. 214-215.

4. Applied Loading Method

Applied loads should be placed along spars or strong ribs of a wing in order to prevent local damage which would not represent the actual aerodynamic loading.

The power source for full scale loading is usually a hydraulic pump. Phase control between pumps is generally obtained by a common oil supply and pressure control. The load is then distributed by a lever system called a whiffletree to many points on the wing. With this lever system one hydraulic cylinder may be used to distribute specified loads at these different loading points on the wing.

Generally the cyclic rate is in the range of ten to thirty per minute for fatigue testing.

For safety a pressure release valve is necessary in case of overloading at peak pressure. A damping unit is generally used to restrict pressure differentials to a rate which will not cause damage to the aircraft. In the event of electrical failure, solenoid valves are designed to revert the pressure control valves to a safe position. Sometimes switches are placed at wing tips to cut the supply of pressure from the hydraulic pump motor should abnormal deflection occur at the wing tips.

5. Testing Procedures

(1) Initially a load should be applied slowly to thoroughly check the system.

(2) Functioning tests are then made to insure correct operation.

(3) Preloading can be applied to induce the effect of occasional severe gusts.

(4) Inspection of the specimen would then be in order.

(5) Adjustment of all switches by use of load cells to insure desired loads is necessary.

(6) Reduction of friction at hydraulic jacks should be kept to a minimum.

(7) Sustain continued 24-hour operation if at all possible.

(8) Periodic inspections of the fatigued specimen should be made. Some inspection may be done during operation. Other checks must be made with the operation stopped and repairs made on the aircraft. Accurate records should be kept of all inspections and repairs.

(9) Continue cyclic loading and repairs until a succession of failures have been produced. Records for these would be needed for service schedules and inspection of aircraft.

C. AIRWORTHINESS REQUIREMENTS AND REGULATIONS

1. Fatigue Requirements

A general requirement is given in the final report of the second session of the ICAO Airworthiness Division (Doc. 3031, Air/181, March 1947, p. 99):

> The strength and fabrication of the aeroplane shall be such as to ensure that the probability of disastrous fatigue failure of the primary structure under repeated loads anticipated in operation is extremely remote during the expected life of the aeroplane or parts thereof. Where a type of construction is used for which experience is not available to show that compliance with static strength requirements will ensure the strength of the structure under repeated loads, its strength under such loads shall be substantiated by suitable investigations.[5]

This requirement recognizes the problem of fatigue but still does not spell out what must be done because the quote "extremely remote

---

[5]ICAO Airworthiness Division (Doc. 3031, Air/181, March 1947, p.99.

possibility" of a failure leading to a disaster does not define responsibility enough for practical use by designers.

Fatigue requirements at present make clear distinction between the safe-life method and the fail-safe design. The requirements seem to be inadequate if just one of the basic methods is used without the other. The following quote seems to support the idea that it is not desirable to have a sharp distinction between safe-life and fail-safe structures:

> ...a reasonable compromise between a rational approach to the problem of safety in fatigue and practicable certification requirements for fail-safe design {must be used}.[6]

Contained in reference (11) is an appendix which considers proposed requirements on fatigue strength in the future. These requirements were prepared in detail by the Netherlands Committee on Structural Strength Requirements for Civil Aircraft, 25 April 1958.

2. Airplane Airworthiness Requirements

a. Load Distribution in the Spanwise Direction

The mean taper ratio is defined as the ratio of the tip chord (obtained by extending the leading and trailing edges to the plane of the wing tip chord) to the root chord (chord at the plane of symmetry or centerline of aircraft when the leading and trailing edges have been extended to this plane of symmetry).

When the mean taper ratio is equal to or greater than 0.5, the following methods and reports are acceptable:

ANC-1(1)

NACA Technical Report 585

NACA TR572

---

[6]W. T. Koiter, "Airworthiness Requirements on Fatigue Strength," Full Scale Fatigue Testing of Aircraft Structures, edited by F. J. Plantema and J. Schijve, Pergamon Press, 1961, p. 386.

If the mean taper ratio is less than 0.5, the span distribution may be determined by rational methods. These methods are used unless known severe distribution exists (4).

b. Load Distribution in the Chord Direction

Approximate methods are generally accepted for chordwise load distribution for testing of wing ribs for conventional two spar construction. The acceptable methods of approximating distributions may be found in references (4) and (5).

Three types of loads are generally considered by aircraft manufacturers on horizontal tail surfaces. They are balancing loads, maneuvering loads, and gust loads. Accepted curves for the distribution of these loading conditions are stipulated in the FAR Part 23, Sections 23.421, 23.423, and 23.425 respectively. For the purposes of this report the balancing load condition was considered, and is covered further in the discussion.

c. Resultant Air Loads on a Wing

Reference (4) gives an acceptable method to determine the points of application of the resultant air load on a wing. A more detailed method which is acceptable is found in ANC-1(3). This method determines the mean effective value of the normal force coefficient, average moment coefficient, location of the mean aerodynamic center, and the value of the mean aerodynamic chord. A simplified version of the tables in this reference can be found in reference (4), Table IV, page 35, for mean taper ratios equal to or greater than 0.5. Also a simplified version can be found in reference (3), page A5.11.

III. DISCUSSION

A. DETERMINING THE AERODYNAMIC LOAD DISTRIBUTION

1. Load Distribution in the Spanwise Direction

For calculating the spanwise lift coefficient ratio, the author used the tables in reference (15). These tables have been developed for numerical computation of the coefficients of the Fourier series method as discussed previously. This method is also called the Lotz method. It was decided to use the tables for ten points along the half span of the stabilator.

Table I gives the necessary geometric characteristics of the Piper stabilator which the author used in the project. The angle of attack, α_a, in this table was assumed to be 1.00. This high positive angle of attack was desired because it represents the high loading condition obtained in a take off attitude at low air speed (16).

The slope of the lift curve versus angle of attack in radians, m_o, was assumed to be 5.67. This value is used throughout the literature and for all practical purposes can be found to be constant for most airfoils.

With the values in Table I known, the B_n coefficients can be calculated. Table II can be used for this purpose. Table II represents the case where the circulation is to be determined at ten different points across the semispan of the wing. The small y_n values in Table II are the coordinates for the $\alpha_a \sin \theta$ curves taken at every 9° (starting with the wing tip at zero) (15).

A numerical check is given at the bottom of Table II. The note at the bottom of Table II applies to the angle of attack condition of the stabilator which the author has used. Thus the computing form for

c	Station	Fraction of Semispan	θ (Deg.)	sin θ	α_a	α_a sin θ	m_o for b=∞	$\frac{m_s}{m_o}$	$\frac{c_s}{c}$	$\frac{m_s c_s}{m_o c}$ sin θ
51.0	10	0.0000	90	1.000	1	1.000	5.67	1.0	1.000	1.000
46.5	9	.1564	81	.988	1	.988	5.67	1.0	1.096	1.073
43.2	8	.3090	72	.951	1	.951	5.67	1.0	1.18	1.122
39.8	7	.4540	63	.891	1	.891	5.67	1.0	1.28	1.140
35.6	6	.5878	54	.809	1	.809	5.67	1.0	1.43	1.157
33.4	5	.7071	45	.707	1	.707	5.67	1.0	1.53	1.081
30.6	4	.8090	36	.588	1	.588	5.67	1.0	1.67	.983
28.0	3	.8910	27	.454	1	.454	5.67	1.0	1.82	.826
26.6	2	.9511	18	.309	1	.309	5.67	1.0	1.91	.590
26.0	1	.9877	9	.156	1	.156	5.67	1.0	1.96	.306
-	0	1.000	0	0	1	0	5.67	1.0	-	-

Table I. Geometric Characteristics of the Piper Stabilator

10 POINTS

y_1 y_2 y_3 y_4 y_5 y_6 y_7 y_8 y_9 $\frac{1}{2}y_{10}$

$y_1+y_3-y_5-y_7+y_9=r_1$ $\qquad\qquad$ $y_2-y_6+\frac{1}{2}y_{10}=r_2$

Multiply	by									
Sin 9=0.1564	y_1		$-y_7$			$-y_3$		y_9		
Sin 18=0.3090		y_2		y_6			y_6		y_2	
Sin 27=0.4540	y_3		y_1			$-y_9$		$-y_7$		
Sin 36=0.5878		y_4		$-y_8$			y_8		$-y_4$	
Sin 45=0.7071	y_5		y_5		r_1	$-y_5$		y_5		
Sin 54=0.8090		y_6		y_2			y_2		y_6	
Sin 63=0.8910	y_7		$-y_9$			y_1		$-y_3$		
Sin 72=0.9511		y_8		y_4			$-y_4$		$-y_8$	
Sin 81=0.9877	y_9		y_3			y_7		y_1		
Sin 90=1.0000		$\frac{1}{2}y_{10}$		$-\frac{1}{2}y_{10}$	r_2		$-\frac{1}{2}y_{10}$		$\frac{1}{2}y_{10}$	
Sum col.1										
Sum col.2										
Col.1+col.2		$=5B_1$		$=5B_3$	$=5B_5$		$=5B_7$		$=5B_9$	
Col.1-col.2		$=5B_{19}$		$=5B_{17}$	$=5B_{15}$		$=5B_{13}$		$=5B_{11}$	

Check: $B_1-B_3+B_5-B_7+B_9-B_{11}+B_{13}-B_{15}+B_{17}-B_{19}=y_{10}$.

Note.-If α_a is constant along the span, $B_1=\alpha_a$ and B_3 to B_{19} are 0.

Table II. Computing Form for Evaluating Angle Coefficients, B_n

the B_n coefficients did not have to be evaluated for the stabilator. Then $B_1 = \alpha_a$ and B_3 to B_{19} are 0.

The computing form for evaluating the Fourier series C_{2n} coefficients can be found in Table III. This table is again designed for ten points across the semispan. The y_n' values are the coordinates of the $\frac{m_s c_s}{m_o c}$ sin θ curves taken at the same intervals as before in Table II (15). Again notice that there is a numerical check found at the bottom of Table III.

Table IV represents the y_n' values of the stabilator substituted into Table III. Also in Table IV is a numerical check and the calculated values of P_n which will be used in Table V.

Table V is the calculating form for the A_n coefficients in the Fourier series equations. This table used the values obtained from Table IV to calculate the A_n coefficients by iterative methods. This form is for the case of the first four harmonics in the Fourier series irrespective of the number of points along the semispan.

In column 1 of Table V are given the operations required to evaluate the coefficients. The tabulated differences of the C_n values are found in column 2. In column 3(a) the values of the A_n coefficients were listed as they became known. Since none of the A_n coefficients were known at the beginning, A_1 was determined as though the others were absent, and is found in column 4(a). The A_3 value was approximated next in column 4(a) in the same way except the value of A_1 just determined could be used. The same method was used to calculate A_5 and A_7. When all of the A_n values had been approximated in column 4(a), they were written in column 3(b) and used except when a new value for the A_n's had

	$\frac{1}{2}y_{10}'$	y_1'	y_2'	y_3'	y_4'	y_5'	v_0	v_1	v_2
		y_9'	y_8'	y_7'	y_6'		v_5	v_4	v_3
Sum	v_0	v_1	v_2	v_3	v_4	v_5	p_0	p_1	p_2
Difference	w_0	w_1	w_2	w_3	w_4		q_0	q_1	q_2

$$10\ C_0 = p_0+p_1+p_2$$
$$5\ C_{10} = w_0-w_2+w_4$$
$$10\ C_{20} = q_0-q_1+q_2$$

Multiply	by							
Sin 18=0.3090	w_4		q_2	p_2	$-w_2$		p_1	$-q_1$
Sin 36=0.5878		w_3				w_1		
Sin 54=0.8090	w_2		q_1	$-p_1$	$-w_4$		$-p_2$	$-q_2$
Sin 72=0.9511		w_1				$-w_3$		
Sin 90=1.00000	w_0		q_0	p_0	w_0		p_0	q_0
Sum col. 1								
Sum col. 2			$=5C_4$	$=5C_{16}$			$=5C_8$	$=5C_{12}$
Col.1+col.2		$=5C_2$				$=5C_6$		
Col.1-col.2		$=5C_{18}$				$=5C_{14}$		

Check: $C_0+C_2+C_4+C_6+C_8+C_{10}+C_{12}+C_{14}+C_{16}+C_{18}+C_{20}=0.$

Table III. Computing Form for Evaluating Plan Form Coefficients, C_{2n}

		0.306	0.590	0.826	0.983	1.081	0.500	1.379	1.712
	0.500	1.073	1.122	1.140	1.157		1.081	2.140	1.966
Sum	0.500	1.379	1.712	1.966	2.140	1.081	1.581	3.519	3.678
Difference	-0.500	-.767	-.532	-.314	-.174		-.581	-.761	-.254

$10\ C_0 = 1.581 + 3.519 + 3.678 = 8.778$
$5\ C_{10} = -.500 + .532\ -.174 = -.142$
$10\ C_{20} = -.581 + .761\ -.254 = -.074$

Multiply	by							
Sin 18 = 0.3090	-.174		-.254	3.678	.532		3.519	.761
Sin 36 = 0.5878		-.314				-.767		
Sin 54 = 0.8090	-.532		-.761	-3.519	.174		-3.678	.254
Sin 72 = 0.9511		-.767				.314		
Sin 90 = 1.000	-.500		-.581	1.581	-.500		1.581	-.581

gives

Sin 18	-.054		-.079	1.138	.164		1.088	.235
Sin 36		-.185				-.451		
Sin 54	-.430		-.616	-2.846	.141		-2.973	.206
Sin 72		-.729				.298		
Sin 90	-.500		-.581	1.581	-.500		1.581	-.581
Sum of Column 1	-.984		-1.276	-.127	-.195		-.304	-.140
Sum of Column 2		-.914	$=5C_4$	$=5C_{16}$		-.153	$=5C_8$	$=5C_{12}$
Col. 1 + Col. 2	$-1.898 = 5C_2$				$-.348 = 5C_6$			
Col. 1 - Col. 2	$-.070 = 5C_{18}$				$-.042 = 5C_{14}$			

(a)

Table IV. Stabilator Calculation Form for the C_{2n} Coefficients

Check: $\sum_{n=0}^{10} C_{2n} = 0$

$C_0 = 0.8778$
$C_2 = -0.3796$
$C_4 = -0.2552$
$C_6 = -0.0696$
$C_8 = -0.0608$
$C_{10} = -0.0284$
$C_{12} = -0.0280$
$C_{14} = -0.0084$
$C_{16} = -0.0254$
$C_{18} = -0.0140$
$C_{20} = -0.0074$

$\sum_{n=0}^{10} = 0.001$

$\simeq 0.00$

$$\frac{c_s m_s}{4b} = \frac{(51)(5.67)}{4(150)} = .482$$

$$P_n = C_0 - \tfrac{1}{2}C_{2n} + n\frac{c_s m_s}{4b}$$

$P_1 = 0.878 - \tfrac{1}{2}(-.380) + 1(.482) = 1.550$

$P_3 = 0.878 - \tfrac{1}{2}(-.070) + 3(.482) = 2.359$

$P_5 = 0.878 - \tfrac{1}{2}(-.0284) + 5(.482) = 3.302$

$P_7 = 0.878 - \tfrac{1}{2}(-.0084) + 7(.482) = 4.691$

(b)

Table IV. Stabilator Calculation Form for the C_{2n} Coefficients

1	2	3(a)	3(b)	3(c)	3(d)	4(a)	4(b)	4(c)	4(d)
$A_3(C_2-C_4)$	-.1244		.0170	.0182	.0184		-.0021	-.0023	-.0023
$A_5(C_4-C_6)$	-.1856		.0160	.0191	.0191		-.0030	-.0035	-.0036
$A_7(C_6-C_8)$	-.0088		.0016	.0017	.0018		-.0000	-.0000	-.0000
Σ						0	-.0051	-.0058	-.0059
$\Sigma/2$						0	-.0025	-.0029	-.0029
$B_1-\Sigma/2$	1.000					1.000	1.0025	1.0029	1.0029
$A_1=\frac{B_1-\Sigma/2}{P_1}$	$\frac{B_1-\Sigma/2}{1.550}$					.645	.647	.647	.647
$A_1(C_2-C_4)$	-.1244	.645	.647	.647	.647	-.080	-.0805	-.0805	-.0805
$A_5(C_2-C_8)$	-.3188		.0160	.0191	.0191		-.0051	-.0061	-.0061
$A_7(C_4-C_{10})$	-.2268		.0016	.0017	.0018		-.0004	-.0004	-.0004
Σ						-.080	-.0860	-.0870	-.0870
$\Sigma/2$						-.040	-.0430	-.0435	-.0435
$B_3-\Sigma/2$	0					.040	.0430	.0435	.0435
$A_3=\frac{B_3-\Sigma/2}{P_3}$	$\frac{B_3-\Sigma/2}{2.359}$					.0170	.0182	.0184	.0184
$A_1(C_4-C_6)$	-.1856	.645	.647	.647	.647	-.120	-.1200	-.1200	-.1200
$A_3(C_2-C_8)$	-.3188	.0170	.0182	.0184	.0184	-.0054	-.0058	-.0059	-.0059
$A_7(C_2-C_{12})$	-.3516		.0016	.0017	.0018		-.0006	-.0006	-.0006
Σ						-.1254	-.1264	-.1265	-.1265
$\Sigma/2$						-.0627	-.0632	-.0632	-.0632
$B_5-\Sigma/2$	0					.0627	.0632	.0632	.0632
$A_5=\frac{B_5-\Sigma/2}{P_5}$	$\frac{B_5-\Sigma/2}{3.302}$					.0160	.0191	.0191	.0191
$A_1(C_6-C_8)$	-.0088	.645	.647	.647	.647	-.0057	-.0057	-.0057	-.0057
$A_3(C_4-C_{10})$	-.2268	.0170	.0182	.0184	.0184	-.0039	-.0041	-.0042	-.0042
$A_5(C_2-C_{12})$	-.3516	.0160	.0191	.0191	.0191	-.0056	-.0067	-.0067	-.0067
Σ						-.0152	-.0165	-.0166	-.0166
$\Sigma/2$						-.0076	-.0082	-.0083	-.0083
$B_7-\Sigma/2$	0					.0076	.0082	.0083	.0083
$A_7=\frac{B_7-\Sigma/2}{P_7}$	$\frac{B_7-\Sigma/2}{4.691}$					.0016	.0017	.0018	.0018

Table V. Stabilator Solution of the A_n Coefficients

been approximated in column 4(b). The complete process was repeated in this table until the A_n values converged (15).

The coefficient of lift, c_ζ, can be found from the equation

$$c_\zeta = \frac{m_s c_s}{c} \Sigma A_n \sin n\theta \tag{25}$$

In determining the load distribution, it is convenient to use a coefficient of lift ratio. This ratio is the lift coefficient at a particular point, c_ζ, divided by the average or constant wing lift coefficient along the entire wing span, C_L. C_L can be defined by the equation

$$C_L = \pi A \frac{m_s c_s}{4b} A_1 \tag{26}$$

In the stabilator example, C_L is equal to 8.22 when an aspect ratio, A, of 8.4, wing area of 2674 sq. in., and a wing span of 150" are used.

Table VI shows the calculations for obtaining the lift coefficient and the corresponding coefficient of lift ratio at various points along the span.

Using the values obtained in Table VI, the shear and the percent of the total load may be found at points along the span in Table VII (3) and (12).

Columns (1) through (4) of Table VII are self-explanatory, the values in column (4) having been taken from Table VI.

	STATION									
	10	9	8	7	6	5	4	3	2	1
θ degrees	90	81	72	63	54	45	36	27	18	9
Sin θ	1.00	.986	.951	.892	.808	.707	.588	.454	.309	.156
Sin 3θ	-1.00	-.892	-.588	-.156	.309	.707	.951	.986	.808	.454
Sin 5θ	1.00	.707	0	-.707	0	-.707	0	.707	1.00	.707
Sin 7θ	-1.00	-.454	.588	.986	.309	-.707	-.951	-.156	.808	.892
$A_1 \sin \theta$	.647	.638	.615	.577	.522	.457	.380	.294	.200	.101
$A_3 \sin 3\theta$	-.0184	-.0164	-.0108	-.0029	.0057	.0130	.0175	.0181	.0149	.0083
$A_5 \sin 5\theta$	.0191	.0135	0	-.0135	0	-.0135	0	.0135	.0191	.0135
$A_7 \sin 7\theta$	-.0018	-.0008	.0011	.0018	.0006	-.0013	-.0017	-.0003	.0015	.0016
$\Sigma A_n \sin n\theta$	.6459	.6343	.6053	.5624	.5283	.4552	.3958	.3253	.2355	.1244
$\frac{m_s c_s}{c}$	5.67	6.21	6.88	7.25	8.11	8.67	9.46	10.3	10.8	11.1
c_l	3.66	3.94	4.17	4.08	4.28	3.95	3.74	3.35	2.55	1.38
$\frac{c_l}{C_L}$	.445	.480	.507	.497	.522	.481	.455	.408	.311	.168

Table VI. Stabilator Computation of the Coefficient of Lift Ratio

(1) Station	(2) Dist. from ℄	(3) c	(4) $\frac{c_l}{C_L}$	(5) h_i	(6) δ_i	(7) $h_i\delta_i$	(8) Δy_i	(9) $\Delta y_i h_i \delta_i$	(10) $R_L h_i \delta_i$	(11) ΔP_z	(12) Shear $\Sigma \Delta P_z$	(13) $\frac{\Delta P_z}{(TL)}$	(14) Dist. from ℄
0	75.0	0.0	.0										
				13.0	.084	1.09	1.0	1.09	.59	.59		≃0	74.5
1	74.0	26.0	.168								.59		
				26.3	.239	6.28	2.8	17.6	3.37	9.43		.0128	72.6
2	71.2	26.6	.311								10.02		
				27.3	.359	9.80	4.5	44.1	5.27	23.7		.0323	68.9
3	66.7	28.0	.408								33.72		
				29.3	.431	12.6	6.2	78.2	6.76	41.8		.0569	63.6
4	60.5	30.6	.455								75.52		
				32.0	.468	15.0	7.5	112.3	8.05	60.4		.0822	56.7
5	53.0	33.4	.481								135.92		
				34.5	.501	17.3	9.0	155.0	9.29	83.6		.114	48.5
6	44.0	35.6	.522								219.52		
				37.7	.509	19.2	10.0	192.0	10.3	103.0		.140	39.0
7	34.0	39.8	.497								322.52		
				41.5	.502	20.8	10.8	225.0	11.2	121.0		.165	28.6
8	23.2	43.2	.507								443.52		
				44.8	.493	22.1	11.4	252.0	11.9	136.0		.185	17.5
9	11.8	46.5	.480								579.52		
				53.7	.462	24.8	11.8	293.0	13.3	157.0		.214	5.9
10	0.0	51.0	.445								736.52		
							Sum =	1370.29					

Assume total load, (TL) = 735#

$$R_L = \frac{(TL)}{\Sigma(\Delta y_i h_i \delta_i)} = \frac{735}{1370.3} = .537\#/in^2$$

Table VII. Stabilator Computation of the Load Distribution

Column (5) is the average value of the chord length at the mid-point between the stations of column (1). The area between the stations of column (1) is called a wing section. Column (6) is the average value of the coefficient of lift ratio at these mid-points. Column (7) is column (5) multiplied by column (6). Column (8) represents the width of a section or the difference between the values in column (2). Column (9) is column (7) multiplied by column (8). The reference lift in psi, R_L, is calculated at the bottom of Table VII. A total load, (TL), was assumed as 735 pounds over the semispan. The sum of column (9) was also used in the calculation of R_L. This value of R_L is multiplied by column (7) to obtain the values in column (10).

Column (11) represents the load acting upon a particular section. Column (11) is Column (8) multiplied by column (10). Column (12) represents the shear force at the ten stations and is the accumulative sum of column (11) starting at the tip of the wing. Notice the last value at station 10 is within slide rule tolerance of the assumed total load. Column (13) represents the percent of the total load at the mid-point of the sections and can be considered the actual spanwise lift distribution at these mid-points.

The equations governing the theory involved in Table VII are as follows:

$$(TL) = (\Delta y_1 h_1)\ (R_L)\ \delta_1 + (\Delta y_2 h_2)\ (R_L)\ \delta_2 + (\Delta y_3 h_3)\ (R_L)\ \delta_3 + \ldots \tag{27}$$

This equation represents the total load or the sum of the loads of each section. The reference lift is represented by Equation 28:

$$R_L = \frac{(TL)}{\Sigma(\Delta y_i h_i \delta_i)} \tag{28}$$

The load or force on each section is evaluated by Equation 29:

$$\Delta P_z = R_L \, h_i \delta_i \, (\Delta y_i) \tag{29}$$

Figure 10 shows the spanwise lift distribution obtained from column 13 of Table VII, using ten points along the span versus the distance from the centerline of the aircraft. This means that the values of the distribution at each of these points should have the sum of 1.00. The requirement which determines a particular load distribution along the span of the wing is the slope of this curve. A curve of the same slope but in a different vertical position will always represent the same load distribution along the wing span if the number of points and/or the location of the points along the span are changed.

In order to compare the slope of this curve to the slope of the curve that Piper Aircraft Corporation apparently used in static tests, the following steps were taken.

Figure 11 shows the pad locations for loading the Piper stabilator for one of the tests by Piper Aircraft Corporation. Only planes A, B,

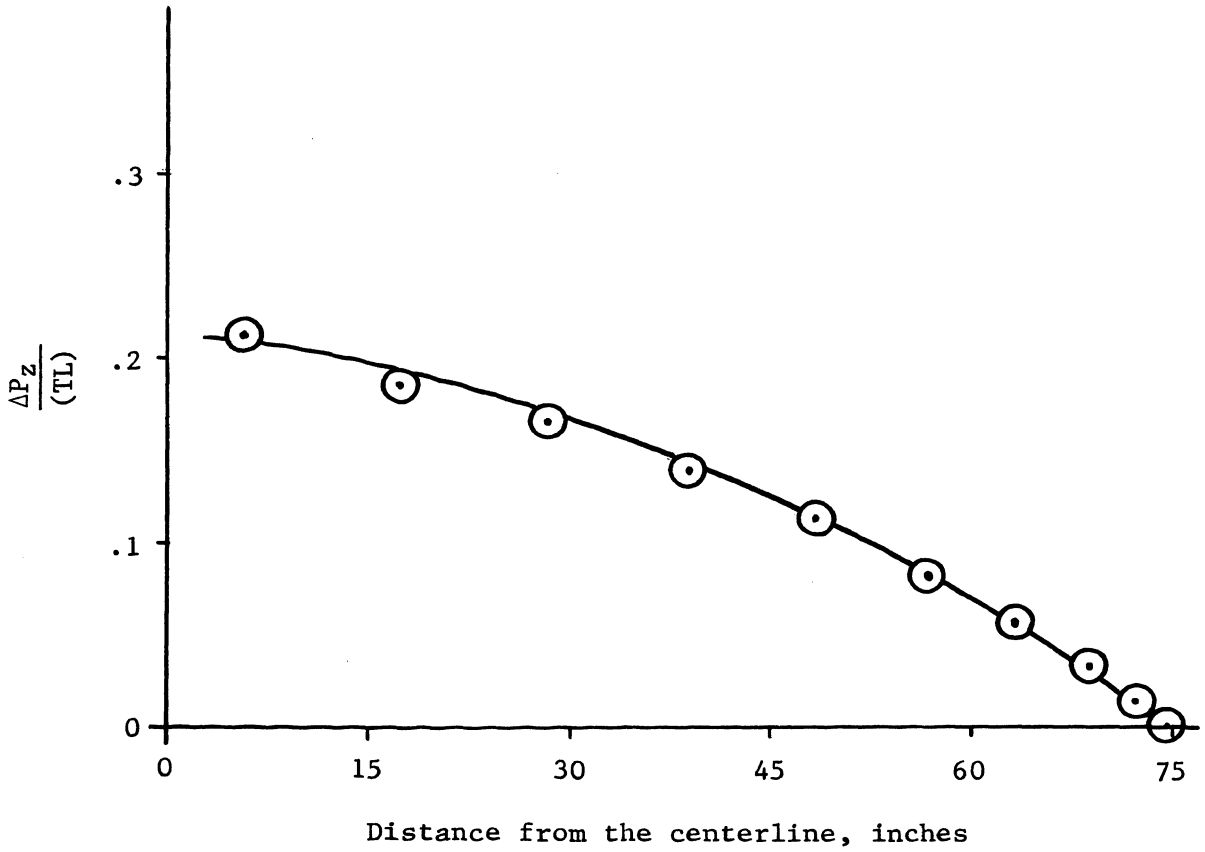

Figure 10. Lift Distribution Obtained from the Fourier Series Analysis

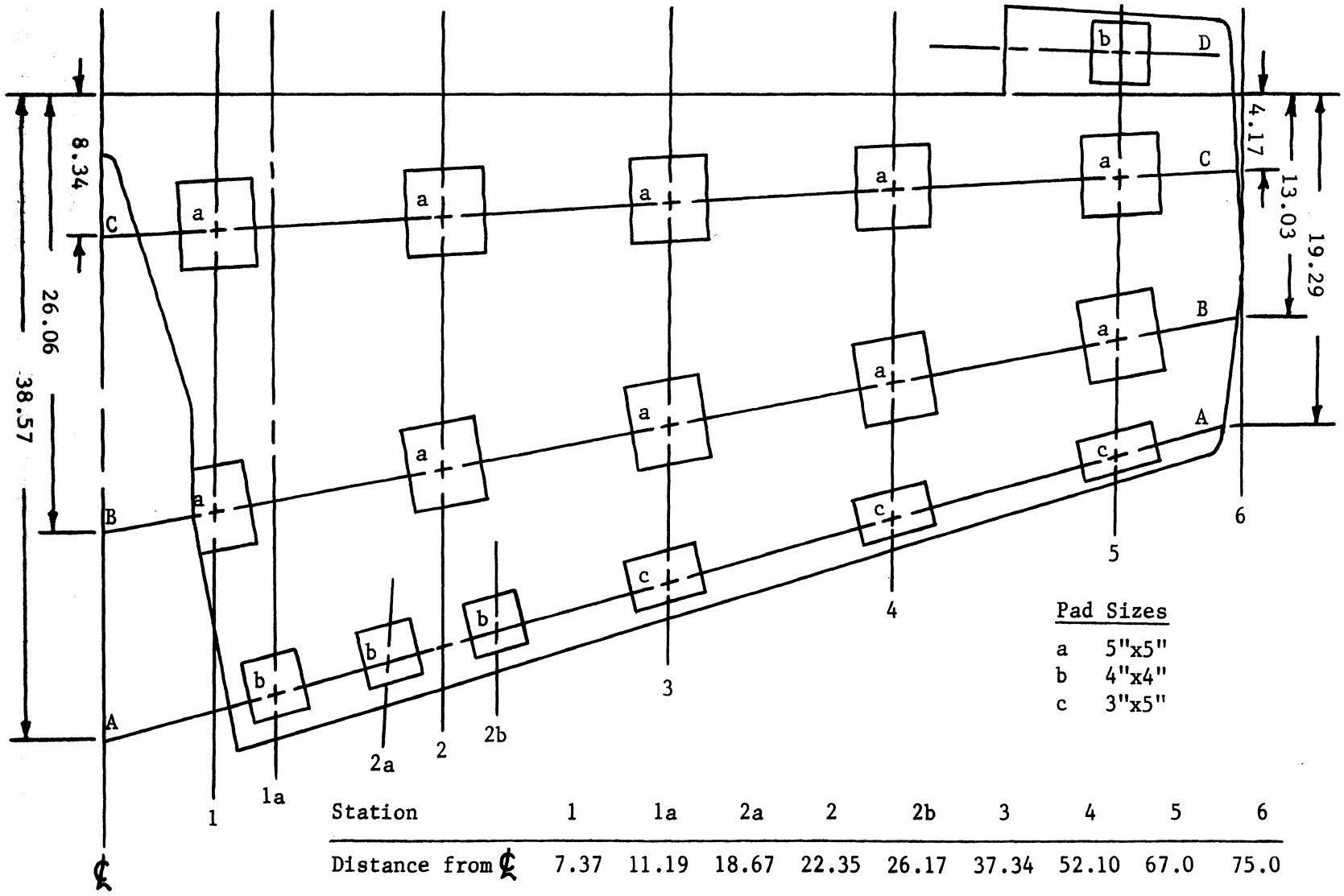

Figure 11. Horizontal Tail Surface Pad Locations Used by Piper Aircraft Corporation

and C will be considered in this report, since the stabilator donated by Piper Aircraft Corporation did not have the antiservo tab included. The spanwise whiffletree design used by Piper is shown in Figure 12, and the corresponding whiffletree dimensions for planes A, B, and C in Figure 11 are given in Table VIII.

The spanwise load distribution obtained from a force analysis of the whiffletree design in the spanwise direction is shown in Table IX. A curve representing the distribution in plane C is shown in Figure 13. Notice that this curve indicates a linear relationship which was apparently used by Piper Aircraft Corporation.

If loading is considered in the C plane and in the exact location of the Piper design having five loading points, the curve in Figure 10 may be transposed vertically up so that the sum of the distribution values at these five points is equal to 1.00. Figure 13 shows the location of the curve with respect to the curve obtained from the Piper analysis. The comparison shows that the Fourier analysis is quite close to the analysis used by Piper Aircraft Corporation for static testing.

The author has used a modified plan from the one designed by Piper Aircraft Corporation in the location of the loading pads on the stabilator. This modified plan is shown in Figure 14. The modification is in plane A near the fuselage. This was done to simplify the whiffletree design and to give a better distribution curve in plane A.

Table X gives the results of the spanwise load distribution in the three planes by transposing the lift distribution curve as described above.

Figure 15 depicts the whiffletree designed by the author for all three planes. Using the values in Table X along with Figures 14 and

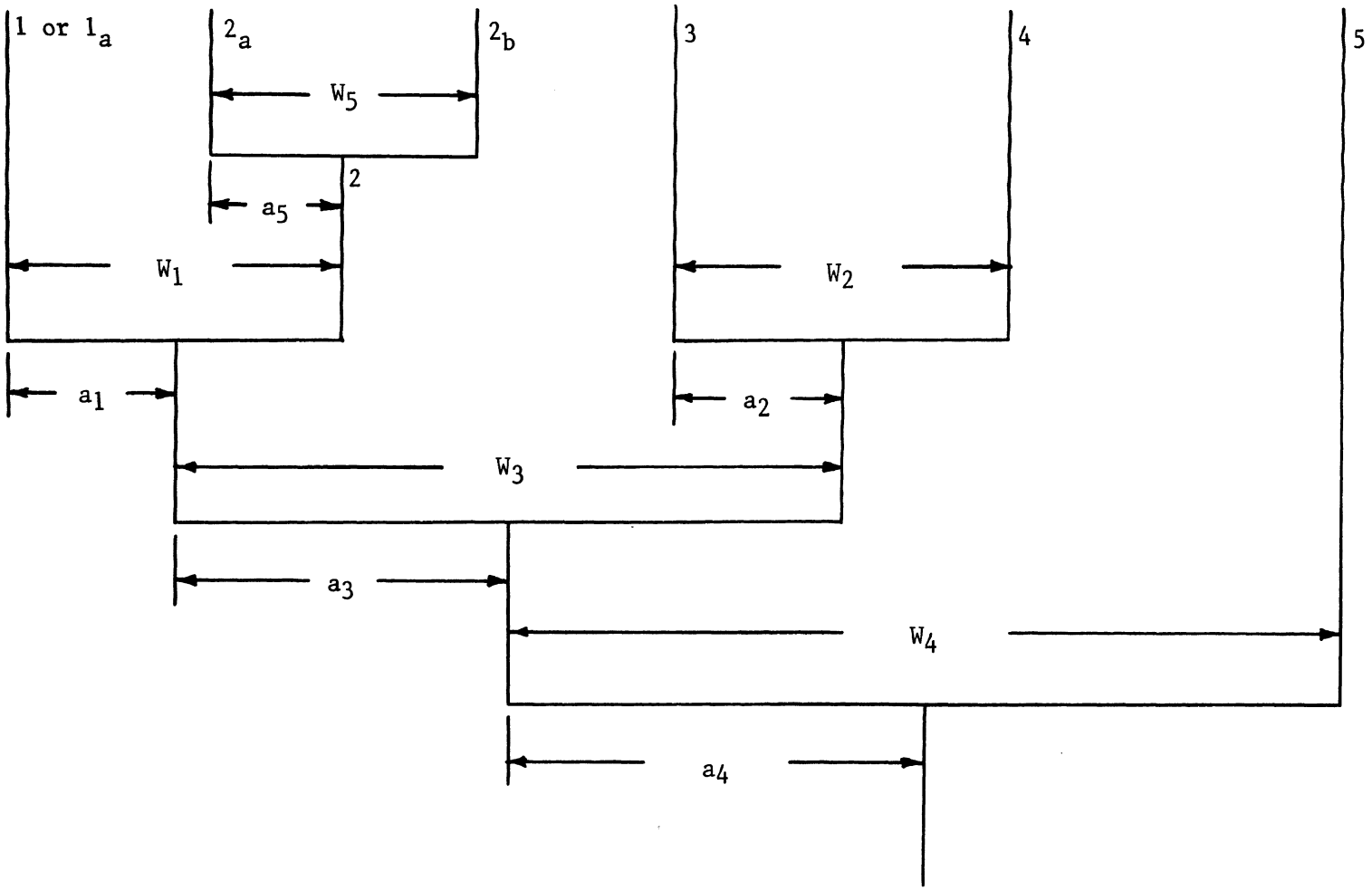

Figure 12. Piper Spanwise Whiffletree Design

Plane	W_1	W_2	W_3	W_4	W_5
A	11.6	15.4	30.8	40.0	7.8
B	15.5	15.1	30.2	40.0	-
C	15.0	15.0	29.6	40.0	-

Plane	a_1	a_2	a_3	a_4	a_5
A	3.4	7.04	13.4	6.1	4.0
B	7.31	6.90	13.12	6.1	-
C	7.07	6.85	12.88	6.1	-

Table VIII. Piper Whiffletree Dimensions

Plane	1	1a	2a	2	2b	3	4	5
A	-	.347	.0733	-	.0694	.194	.162	.153
B	.252	-	-	.226	-	.200	.169	.153
C	.252	-	-	.226	-	.200	.169	.153

Table IX. Piper Design of the Spanwise Load Distribution

Plane	1	1a	2a	2	2b	3	4	5
A	-	.265	-	.245	-	.214	.165	.106
B	.270	-	-	.245	-	.214	.165	.106
C	.270	-	-	.245	-	.214	.165	.106

Table X. Thesis Project Design of the Spanwise Load Distribution

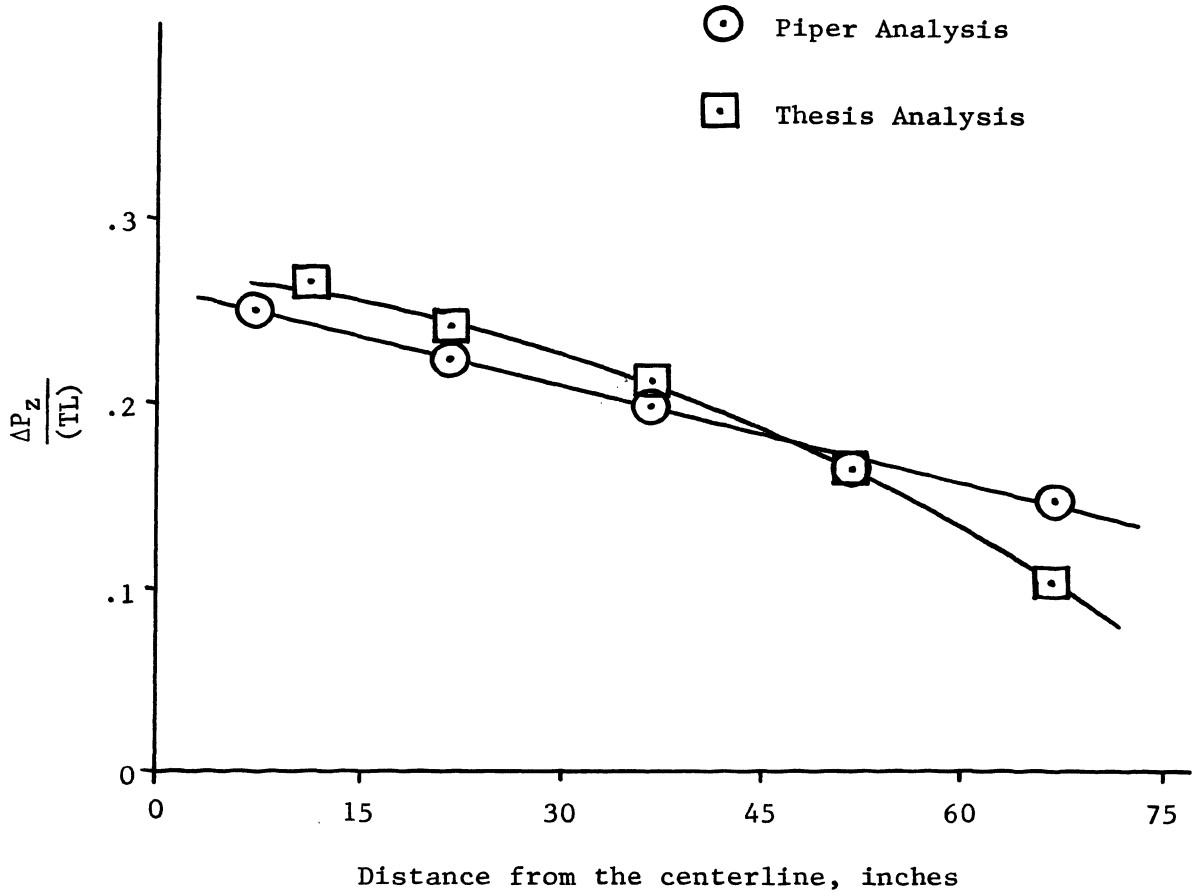

Figure 13. Comparison of Lift Distribution in Plane C

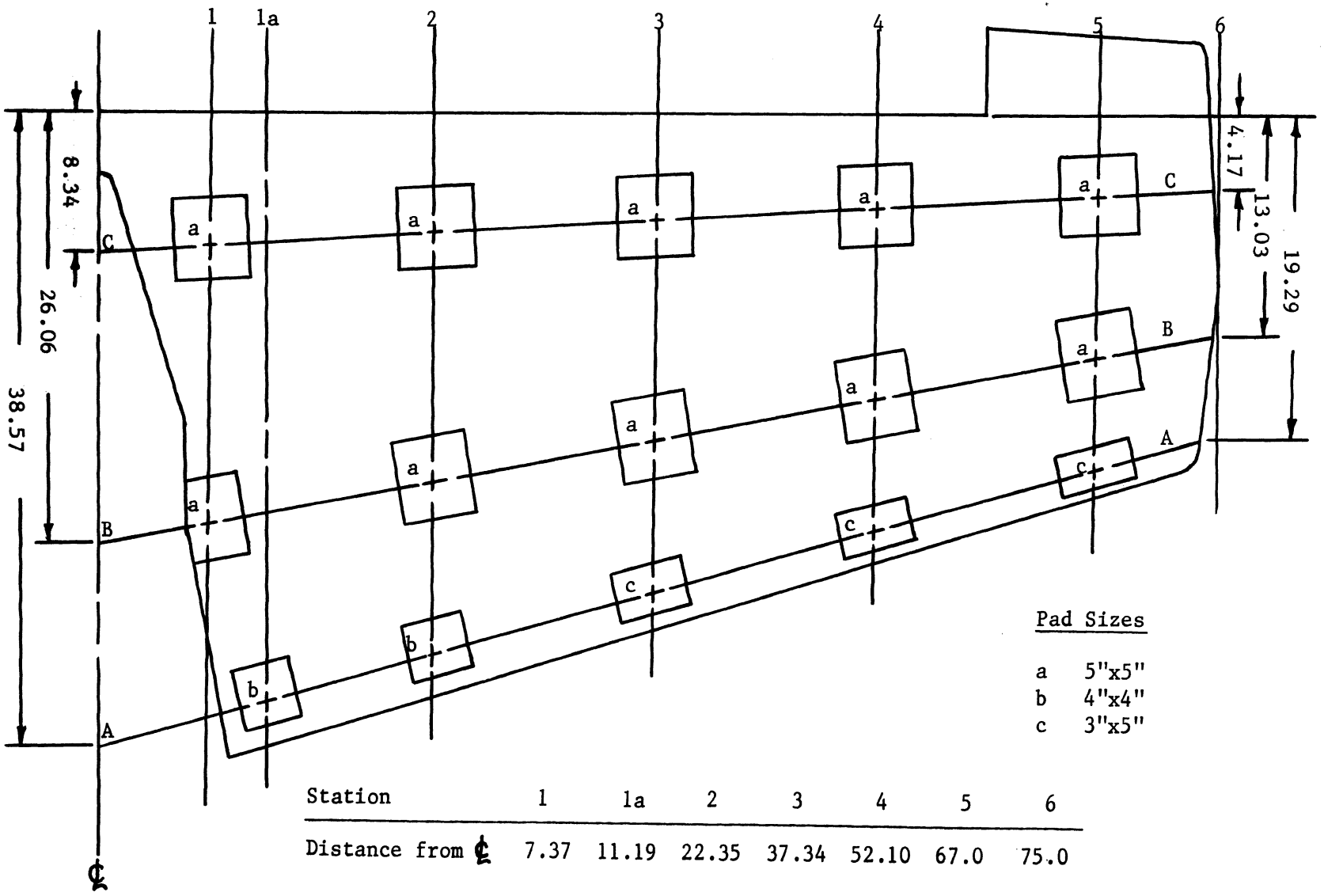

Figure 14. Stabilator Pad Locations Used in the Thesis Project

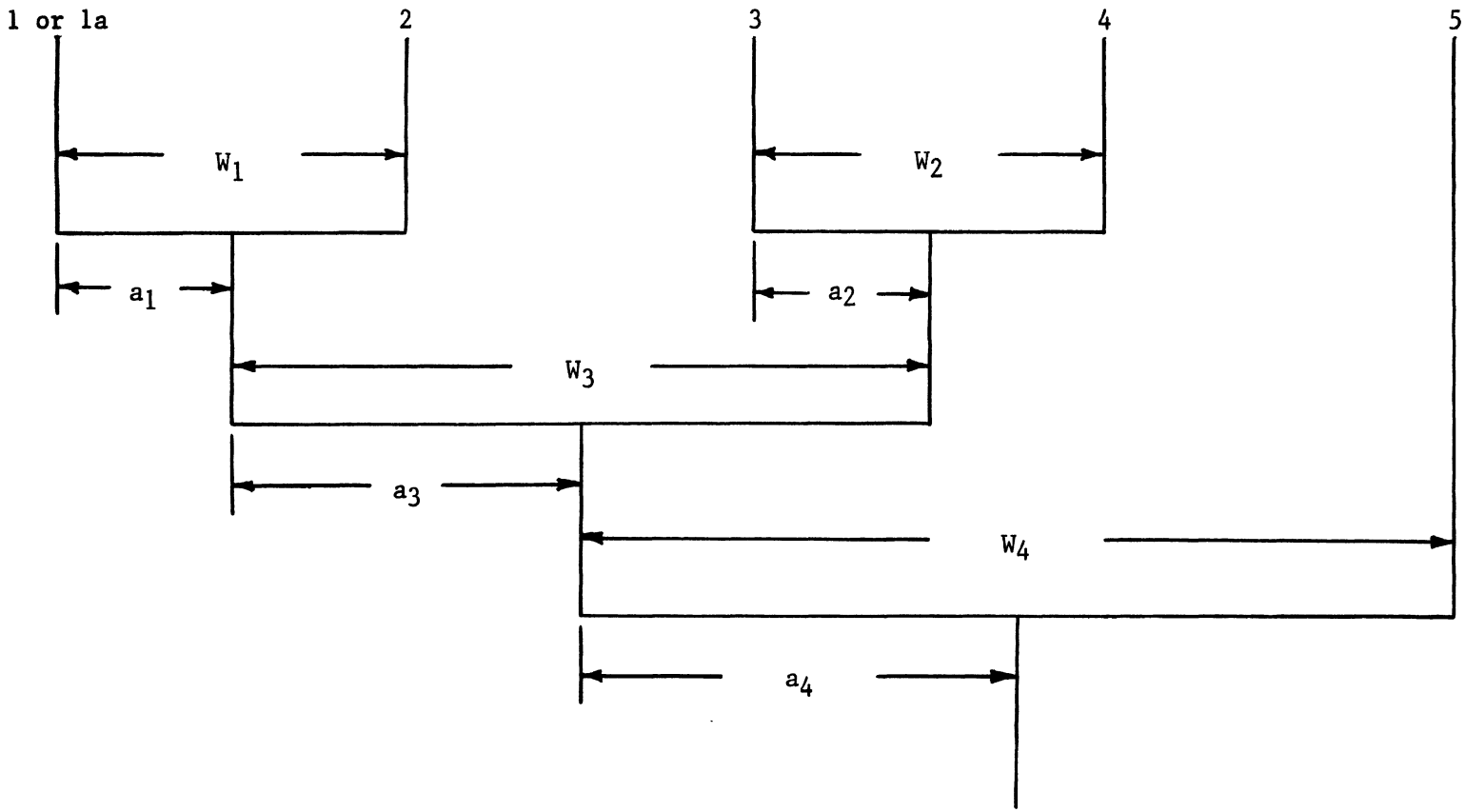

Figure 15. Thesis Whiffletree Design

15, a force analysis was made to obtain the dimensions of the whiffle-tree system to be used in the thesis project. These dimensions are compiled in Table XI.

2. Load Distribution in the Chord Direction

The author has used the balancing load condition as formulated by the Federal Aviation Regulations, Part 23. This horizontal tail balancing load is needed to maintain equilibrium in a flight condition with no pitching present. The balancing condition was chosen because it represented more closely the loading criteria in the take off attitude.

The computation form for the chordwise distribution is Table XII. It uses Figure 16 and an assumed chord length of 33" to compute the load percentage in each section of Figure 16. The planes A, B, and C of Figure 14 fall within the three sections of Figure 16. Thus a corresponding chordwise distribution can be found in planes A, B, and C.

B. STABILATOR TEST CONSTRUCTION

1. Stabilator Mounting

The stabilator was mounted to an H-column in the Mechanical Engineering Department Laboratory. A thick-walled pipe was partially turned down on one end to fit into the fittings of the stabilator. The other end of the 18" long pipe was squared off and welded to the center of a 1/2" thick rectangular steel plate. The steel plate was then bolted to the flange of the H-column with six 1/2" diameter bolts. The stabilator was bolted to the pipe in a horizontal position. A photograph of the stabilator test system is shown in Figure 17.

Plane	W_1	W_2	W_3	W_4
A	11.52	15.22	28.11	40.09
B	15.25	15.00	29.75	40.72
C	15.00	14.75	29.29	40.09

Plane	a_1	a_2	a_3	a_4
A	5.53	6.64	12.00	4.28
B	7.25	6.53	12.60	5.00
C	7.14	6.43	12.42	4.25

Table XI. Thesis Whiffletree Dimensions

Assume c = 33"

.15c = 4.95"
.45c = 14.85"
.40c = 13.2"

$$3w(4.95) = 14.86w$$
$$2w(14.85) = 29.7w$$
$$w(13.2) = \underline{13.2w}$$
$$57.76w$$

P	D	
A	.257	P: Spanwise plane
B	.514	
C	.229	D: Chord distribution

Table XII. Computation Form for the Chordwise Distribution

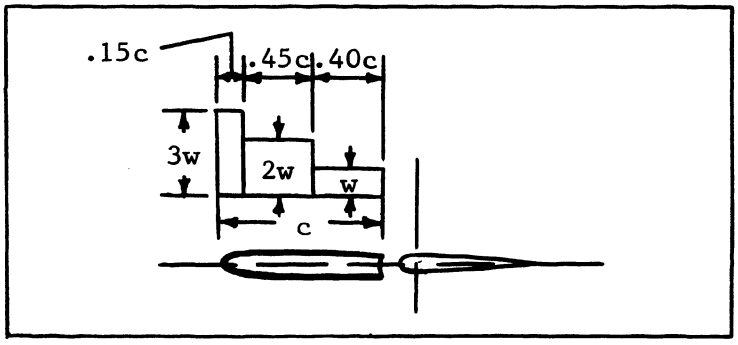

$$w = \frac{\text{Load on fixed surface}}{1.75 \text{ Area of fixed surface}}$$

Figure 16. Tail Surface Load Distribution in the Chord Direction

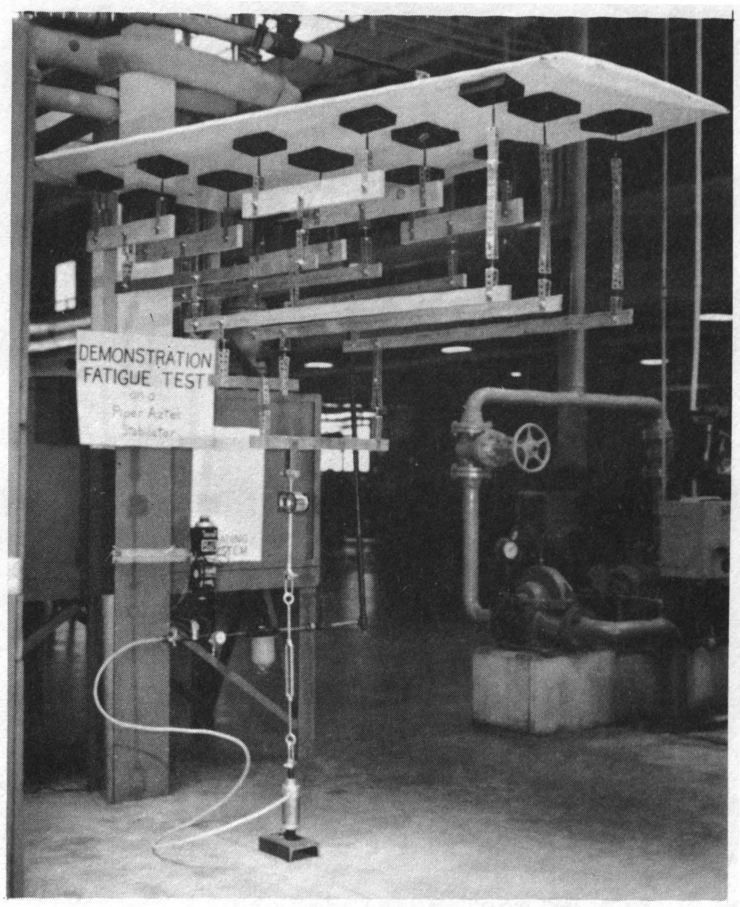

Figure 17. Stabilator Test System

2. Whiffletree Design

The loading pads will first be considered. 1" thick rubber was cut to the sizes shown in Figure 14. These pads were then drilled to allow passage of a steel cable through the center. A 1-1/4" diameter washer was countersunk into the rubber pad and connected to the end of the steel cable passing through it. The pads were then glued with contact cement to the stabilator with the countersunk hole against the surface, in the proper locations as indicated in Figure 14. This pad design is a combination of the methods used by Piper Aircraft Corporation and Beechcraft Aircraft Corporation.

The connecting bars in the top tier were made of wood. All of the other connecting bars in the lower tiers were made of aluminum. The loading connectors between the tiers were made of galvanized steel strapping. Figure 18 is a photograph of the whiffletree system and the loading pads.

Figure 18. Whiffletree System

3. Loading System and Control

Figure 19 is a flow chart of the pressure control system for loading. A 2" bore reversible single acting air cylinder was used to load the whiffletree system. The air cylinder was driven by an air compressor. An air line regulator was used to control the output pressure, thus controlling the amount of load applied to the whiffletree system.

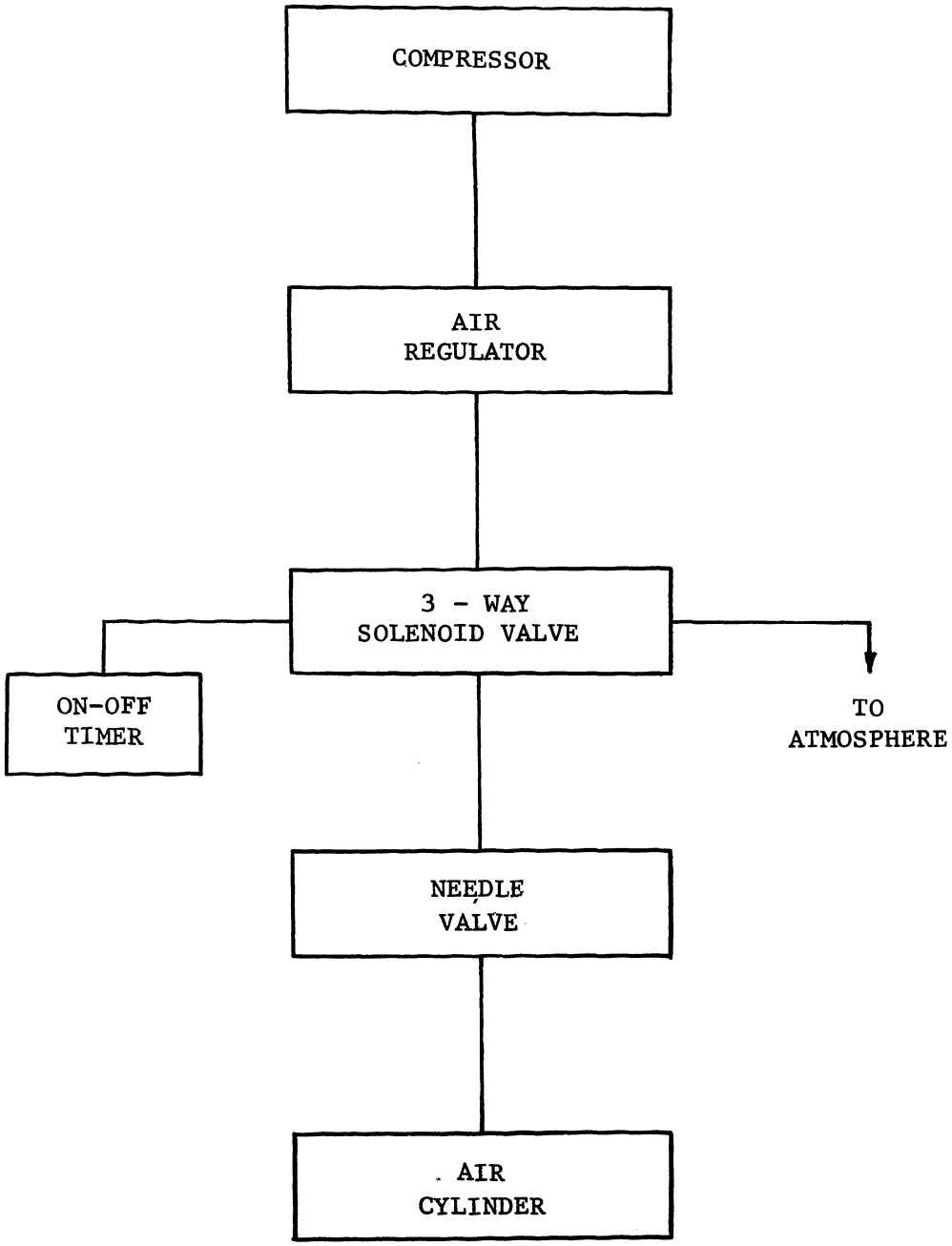

Figure 19. Pressure Control System

An air line filter was used to eliminate water and oil from the shop air supply.

An on-off repeat cycle timer was used to control the time of loading and unloading of the system. The timer controlled a three-way solenoid valve which opened or closed the air supply to the air cylinder and allowed the air to escape to the atmosphere on the off-portion of the cycle.

A needle valve was used between the solenoid valve and the air cylinder for flow adjustment to restrict an undesired rapid rate of loading or unloading.

Figure 20 is a photograph of the control loading system.

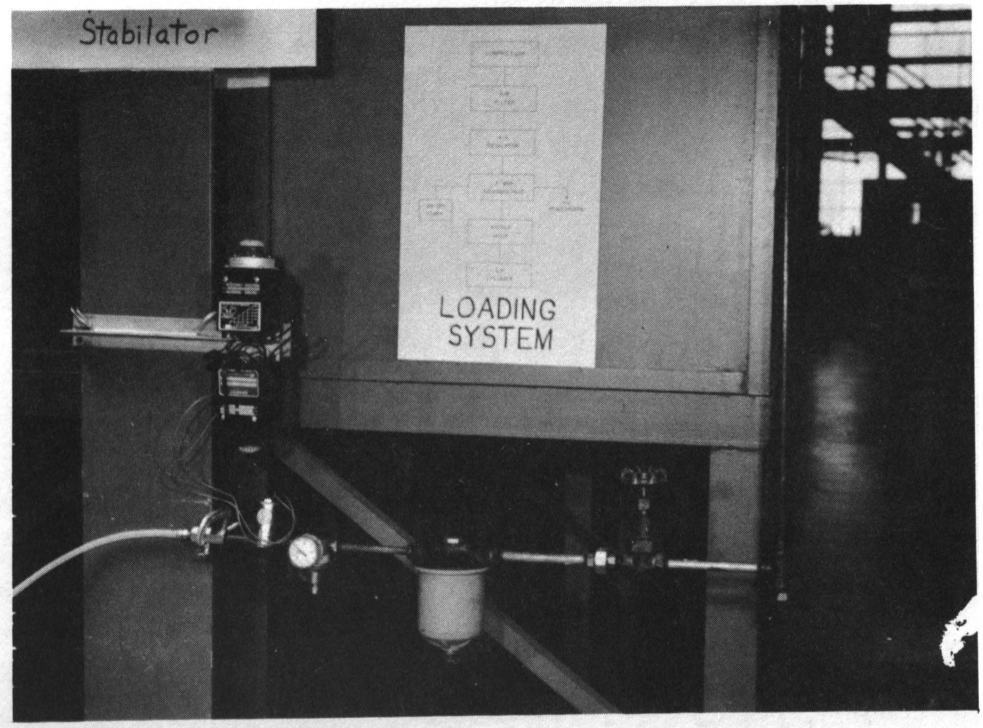

Figure 20. Control Loading System

Figure 21 is a photograph of the air cylinder used to load the whiffletree system.

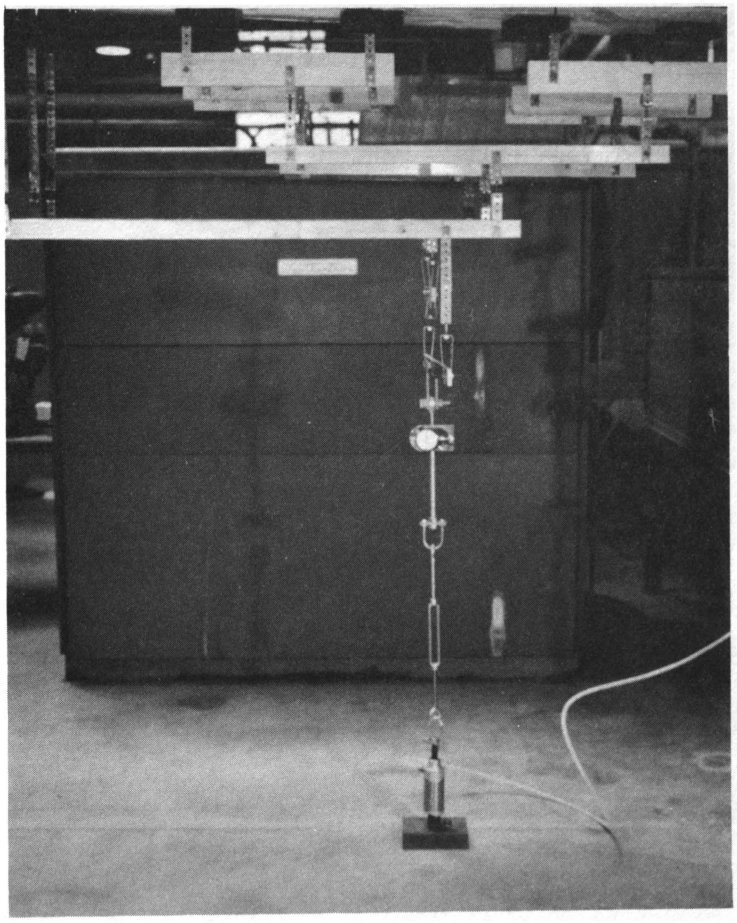

Figure 21. Loading Air Cylinder and Whiffletree

IV. CONCLUSIONS AND RECOMMENDATIONS

The fatigue test which has been designed and constructed should serve well as a laboratory demonstration apparatus. In addition an actual fatigue test could be run if this were deemed desirable.

If an actual fatigue test were to be run, further study in the type of epoxy used for gluing the pads to the wing structure should be done since in actual testing the loading would be greater. Also because of higher loading, a larger air cylinder or possibly a hydraulic cylinder of the double acting type would be necessary. The galvanized steel strapping between the tiers might have to be replaced by a heavier material in order to eliminate fatigue failures of the strapping. Different chordwise distributions could also be tested using the maneuvering or gust loading conditions set up by Federal Aviation Regulations, Part 23.

The Fourier method for obtaining the spanwise lift distribution has been described in detail. This method is exact in the sense that a series can be exact and it applies for a wing with any plan form.

Comparison of the spanwise lift distribution to the approximation used by Piper Aircraft Corporation for static tests showed a very close relationship. The Fourier method indicated that this distribution would be a curve. The actual lift distribution would not be a linear relationship, as was apparently used by Piper Aircraft Corporation. However, a linear relationship can be considered a very close approximation of the actual distribution, and thus justify its use.

V. BIBLIOGRAPHY

1. ANC-1(1), "Spanwise Air-load Distribution," Army-Navy-Commerce Committee on Aircraft Requirements, 1938.

2. ANC-1(3), "Chordwise Air Load Distribution of Airfoils," Army-Navy-Commerce Committee on Aircraft Requirements, (date not available).

3. Bruhn, E. F., Analysis and Design of Flight Vehicle Structures, Tri-State Offset Company, Cincinnati, Ohio, 1965.

4. "Civil Aeronautics Manual," Part 04, Appendix V, U. S. Department of Commerce, Civil Aeronautics Administration.

5. Federal Aviation Regulations, Part 23.

6. Garrison, Peter, "Stabilators," Flying (magazine), January, 1970.

7. Glauert, H., The Elements of Aerofoil and Airscrew Theory, Cambridge University Press, London, 1926.

8. Hardrath, Herbert F., "Current Trends in Fatigue Tests of Aircraft," Full Scale Fatigue Testing of Aircraft Structures, edited by F. J. Plantema and J. Schijve, Pergamon Press, 1961.

9. Huston, Wilbur B., "Comparison of Constant-Level and Randomized-Step Tests of Full-Scale Structures as Indicators of Fatigue-Critical Components," Full Scale Fatigue Testing of Aircraft Structures, edited by F. J. Plantema and J. Schijve, Pergamon Press, 1961.

10. ICAO Airworthiness Division, Document 3031, Air/181, March, 1947.

11. Koiter, W. T., "Airworthiness Requirements on Fatigue Strength," Full Scale Fatigue Testing of Aircraft Structures, edited by F. J. Plantema and J. Schijve, Pergamon Press, 1961.

12. Lehnhoff, T. F., AE 283 Aerospace Structures, Class Notes, 1969.

13. Locati, L., and Sarzotti, G., "Fatigue Ratio as Design Evaluation of Aircraft Structures," Full Scale Fatigue Testing of Aircraft Structures, edited by F. J. Plantema and J. Schijve, Pergamon Press, 1961.

14. Lotz, Irmgard, "Berechnung der Auftriebsverteilung beliebig geformter Flugel, Z. Flugtech. u. Motorluftschiffahrt, Vol. 22, No. 7, April 14, 1931.

15. Pearson, H. A., "Span Load Distribution for Tapered Wings with Partial Span Flaps," NACA TR 585, 1937.

16. Peery, David J., Aircraft Structures, McGraw-Hill Book Company, Inc., 1950.

17. Schrenk, O., A Simple Approximation Method for Obtaining the Spanwise Lift Distribution, NACA TM 948, 1940.

18. Shenstone, B. S., "The Lotz Method for Calculating the Aerodynamic Characteristics of Wings," R.A.S. Journal, Vol. XXXVIII, No. 281, May 1934.

19. Winkworth, W. J., "The Fatigue Testing of Aircraft Structures," Full Scale Fatigue Testing of Aircraft Structures, edited by F. J. Plantema and J. Schijve, Pergamon Press, 1961.

VI. VITA

Stephen Andrew Wright was born on January 15, 1945, in Kansas City, Missouri. He received his first three years of primary school in Kansas City, Missouri. He obtained the remaining portion of his primary and secondary education in the St. Louis area. He entered the University of Missouri - Rolla in September, 1963. He received a Bachelor of Science degree in Mechanical Engineering from the University of Missouri - Rolla, in Rolla, Missouri, in January, 1968.

The author enrolled in the Graduate School of the University of Missouri - Rolla after obtaining his Bachelor of Science degree. He was married on January 4, 1969. He was a graduate assistant for two years while working toward his Master of Science degree.